Deciphering petrogenic processes using Pb isotope ratios from time-series samples at Bezymianny and Klyuchevskoy volcanoes, Central Kamchatka Depression

Massachusetts Institute of Technology

ORIGINAL PAPER

Deciphering petrogenic processes using Pb isotope ratios from time-series samples at Bezymianny and Klyuchevskoy volcanoes, Central Kamchatka Depression

Theresa M. Kayzar · Bruce K. Nelson ·
Olivier Bachmann · Ann M. Bauer · Pavel E. Izbekov

Abstract The Klyuchevskoy group of volcanoes in the Kamchatka arc erupts compositionally diverse magmas (high-Mg basalts to dacites) over small spatial scales. New high-precision Pb isotope data from modern juvenile (1956–present) erupted products and hosted enclaves and xenoliths from Bezymianny volcano reveal that Bezymianny and Klyuchevskoy volcanoes, separated by only 9 km, undergo varying degrees of crustal processing through independent crustal columns. Lead isotope compositions of Klyuchevskoy basalts–basaltic andesites are more radiogenic than Bezymianny andesites ($^{208}Pb/^{204}Pb = 37.850$–37.903, $^{207}Pb/^{204}Pb = 15.468$–15.480, and $^{206}Pb/^{204}Pb = 18.249$–18.278 at Bezymianny; $^{208}Pb/^{204}Pb = 37.907$–37.949, $^{207}Pb/^{204}Pb = 15.478$–15.487, and $^{206}Pb/^{204}Pb = 18.289$–18.305 at Klyuchevskoy). A mid-crustal xenolith with a crystallization pressure of 5.2 ± 0.6 kbars inferred from two-pyroxene geobarometry and basaltic andesite enclaves from Bezymianny record less radiogenic Pb isotope compositions than their host magmas. Hence, assimilation of such lithologies in the middle or lower crust can explain the Pb isotope data in Bezymianny andesites, although a component of magma mixing with less radiogenic mafic recharge magmas and possible mantle heterogeneity cannot be excluded. Lead isotope compositions for the Klyuchevskoy Group are less radiogenic than other arc segments (Karymsky—Eastern Volcanic Zone; Shiveluch—Northern Central Kamchatka Depression), which indicate increased lower-crustal assimilation beneath the Klyuchevskoy Group. Decadal timescale Pb isotope variations at Klyuchevskoy demonstrate rapid changes in the magnitude of assimilation at a volcanic center. Lead isotope data coupled with trace element data reflect the influence of crustal processes on magma compositions even in thin mafic volcanic arcs.

Keywords Assimilation · Kamchatka · Magma mixing · Pb isotopes · Trace element · Major element

T. M. Kayzar (✉) · B. K. Nelson · O. Bachmann · A. M. Bauer
Department of Earth and Space Sciences, University
of Washington, Seattle, WA 98195, USA
e-mail: kayzar1@llnl.gov; tkayzar@gmail.com

T. M. Kayzar
Lawrence Livermore National Laboratory, U.S. Department
of Energy, Livermore, CA 94550, USA

O. Bachmann
Department of Earth Sciences, Institute of Geochemistry
and Petrology, ETH Zurich, Clausiusstrasse 25, 8092 Zurich,
Switzerland

A. M. Bauer
Earth, Atmospheric and Planetary Sciences, Massachusetts
Institute of Technology, Cambridge, MA 02139, USA

P. E. Izbekov
Geophysical Institute, University of Alaska, Fairbanks,
AK 99775, USA

Introduction

The generation of compositional diversity in igneous rocks on small spatial scales within a volcanic arc, or within single volcanoes, is a complex problem of petrology and geochemistry. Compositional variation can result from fractional crystallization, assimilation, magma mixing, or

source heterogeneity—mechanisms that may be difficult to disentangle on a geochemical basis, especially for arcs constructed on relatively juvenile crust. The Klyuchevskoy Group of the Kamchatka arc is a unique arc end-member within which the origin of compositional variation in magmatic suites may be investigated with less ambiguity due to a relatively limited number of geochemical components in this region. Volcanoes in the Klyuchevskoy Group erupt magmas with MORB-like isotopic signatures (Kepezhinskas et al. 1997), the crust is ~35 km thick (Balesta 1991), and subducted sediment input to magma generation is less than 1 % (Kersting and Arculus 1995). Additionally, the Klyuchevskoy Group of volcanoes is composed of twelve different volcanic centers within ~100 km of one another that erupt a range of compositions allowing for the investigation of temporal compositional change.

Two volcanoes within the Klyuchevskoy Group, Bezymianny and Klyuchevskoy, are separated by only 9 km and erupt magmas with compositions that range from high-magnesium basalts to dacites. These systems erupt frequently, permitting the investigation of compositional variation on both short temporal and spatial scales. The petrology and chemistry of Klyuchevskoy volcano have been well studied (Khrenov et al. 1991; Kersting and Arculus 1994; Khubanaya et al. 1994; Ariskin et al. 1995; Ozerov et al. 1997; Khubanaya and Sobolev 1998; Pineau et al. 1999; Dorendorf et al. 2000; Ozerov 2000; Volynets et al. 2000; Dosseto et al. 2003; Mironov et al. 2001; Portnyagin et al. 2007a, b; Turner et al. 2007; Auer et al. 2009; Mironov and Portnyagin 2011). However, Bezymianny volcano, which erupts the most silicic melts in the Klyuchevskoy Group, has not been as well characterized geochemically. Ozerov et al. (1997) suggested that Klyuchevskoy and Bezymianny are genetically related, which is supported by overlapping stable (O) and radiogenic (Pb, Nd) isotope data for the two systems (Kersting and Arculus 1995; Pineau et al. 1999; Dorendorf et al. 2000; Churikova et al. 2001; Bindeman et al. 2004; Münker et al. 2004), but recent studies show evidence for magma mixing (Almeev et al. 2013a; Shcherbakov et al. 2011; Turner et al. 2013) and an independent link to a mantle velocity anomaly at Bezymianny (Koulakov et al. 2013).

Most studies of volcanism in Kamchatka tend to be arc-length in scale (Hochstaedter et al. 1996; Kepezhinskas et al. 1997; Churikova et al. 2001; Ishikawa et al. 2001; Tolstykh et al. 2003; Bindeman et al. 2004; Portnyagin et al. 2005) or focused on one volcano, e.g., Klyuchevskoy (cited above). There are few studies that provide detailed sampling of modern eruptions that allow the comparison of one magmatic system to another within the Klyuchevskoy Group (Ozerov et al. 1997; Dosseto et al. 2003; Turner et al. 2007). We present new data from dense sampling of

Bezymianny volcano that includes older extrusive domes, modern eruptive products, and enclaves and xenoliths brought to the surface in modern erupted magmas. We use high-precision multiple collector inductively coupled plasma mass spectrometry (MC–ICP–MS) Pb isotope data to test hypotheses for the source of magmatism in the Klyuchevskoy Group, the extent of crustal involvement or modification of magmas, and the degree of geochemical contamination in melting source. We couple isotopic compositions with major and trace element characterization of Bezymianny to model how magmas erupted from Bezymianny and Klyuchevskoy volcanoes relate to each other. The data presented here provide evidence for the preservation of small spatial scale compositional variations between the adjacent magmatic systems.

Background and geologic setting

The 80–90 Ma oceanic crust of the northwest corner of the Pacific plate subducts at a rate of 8–9 cm/year beneath accreted Mesozoic and Tertiary mafic volcanic terranes to form the Kamchatka Volcanic Arc (Minster and Jordan 1978; Watson and Fujita 1985; Gorbatov et al. 1997; Konstantinovskaia 2001). Volcanic vents align along three segments: the Eastern Volcanic Front (EVF), the Central Kamchatka Depression (CKD) and the Sredinny Ridge (SR) (Fig. 1). With over 25 active volcanic centers, the Kamchatka Volcanic Arc is the most productive arc on Earth (Fedotov et al. 1991; Melekestsev et al. 1991; Churikova et al. 2001).

The Klyuchevskoy Group of volcanoes (KG) resides within the CKD, which is a large graben resulting from intra-arc rifting that is approximately 350 km in length by 5–100 km in width (Kepezhinskas et al. 1997). Twelve volcanic centers comprise the volcanism in the KG, of which Bezymianny and Klyuchevskoy are the most active (Melekestsev et al. 1991). The subducting slab is located at a depth between 150 and 200 km beneath the KG (Gorbatov et al. 1997; Portnyagin and Manea 2008). The composition of the crust beneath these volcanoes is uncertain and proposed to consist of Cenozoic volcanic deposits to 8 km depth, below which mafic crust at greenschist and/or amphibolite metamorphic facies extends to depths of ~30 km (Fedotov et al. 1991; Dorendorf et al. 2000). Approximately 300 km south, beneath eastern Kamchatka, the amphibolitic Ganal Massif outcrops and represents the closest exposed analog for the lower crust in Kamchatka. The Ganal Massif developed approximately 66 Ma and accreted ~24 Ma (Bindeman et al. 2002). The total thickness of crust beneath the CKD is 30–40 km with the region from ~25 to 40 km representing a 10–12-km-thick
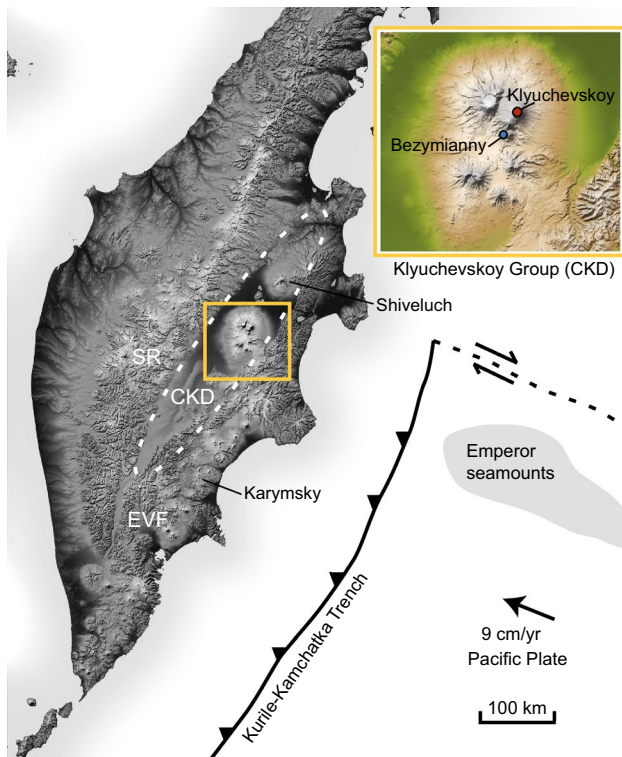
Fig. 1 Tectonic map of the Kamchatka Peninsula showing the location of the Klyuchevskoy group of volcanoes within the Central Kamchatka Depression—CKD. The CKD is shown by a white dotted line. Other volcanic segments in Kamchatka are labeled (Eastern Volcanic Front—EVF, and the Sredinny Range—SR. *Inset* Klyuchevskoy Group of volcanoes. *Colored circles in the inset* denote volcanoes in this study (*red* Klyuchevskoy, *blue* Bezymianny)). The locations of Shiveluch volcano in the Northern CKD and Karymsky volcano in the EVF are also shown for reference

crust–mantle transition interpreted as deep ponding of basaltic magmas generated in the mantle wedge (Balesta 1991; Lees 2007). Magmatism in the CKD is a product of partial melting of a depleted mantle source that has been metasomatized by hydrous slab-derived fluids with possible chemical contributions from altered oceanic crust associated with the emperor seamount chain (Dorendorf et al. 2000; Portnyagin et al. 2007b). Decompression melting may occur beneath the extinct Sredinny Range to the west of the CKD as well as north of the Klyuchevskoy Group (Yogodzinski et al. 2001; Portnyagin et al. 2005, 2007b; Volynets et al. 2010). If decompression melting occurs in the CKD, its signature is strongly masked by fluid-fluxed melting in the wedge (Churikova et al. 2001).

Isotope systematics (Pb, Nd) and major element trends of the CKD constrain the amount of assimilation of subducted sediment and crust by melts of the mantle wedge. A strong MORB-like signature in Nd and Pb isotopes is observed in products from Bezymianny and Klyuchevskoy

(Kersting and Arculus 1995; Kepezhinskas et al. 1997; Dorendorf et al. 2000; Churikova et al. 2001; Pb isotope data in this study). Lead isotope compositions of sediments from the ODP Leg 145 Site 881, 883, and 884 drill cores from the Pacific Ocean off the coast of Kamchatka limit subducted sediment input into the arc to less than 1 % (Kersting and Arculus 1995). In addition, the primitive nature of melts (Mg# 71 at Klyuchevskoy: KLU-16 from Dorendorf et al. 2000) suggests limited crustal assimilation (Pineau et al. 1999; Dorendorf et al. 2000; Ishikawa et al. 2001). Oxygen isotope data, however, suggest that large amounts of assimilation may occur beneath the CKD, but the required assimilant is altered lithospheric mantle that would not modify Mg values (Auer et al. 2009).

Klyuchevskoy and Bezymianny volcanic systems

Klyuchevskoy volcano is the most voluminous mafic arc volcano in the world, erupting $\sim$55 $\times$ 10^6 t/year of high-Mg basalt and high-Al basaltic andesite (Melekestsev et al. 1991). Activity prior to 1932 was focused primarily in the central vent region of the volcano. However, after 1932, numerous flank eruptions occurred (Ozerov et al. 1997). Eruptions last from weeks to years and range in style including vulcanian, strombolian, lava fountaining and lava flows. Sub-plinian events occur at Klyuchevskoy, but are rare, with the last observed event in October 1994 (Ozerov 2000).

Bezymianny is the only active volcano in the KG that erupts dominantly andesite. Following a catastrophic lateral blast eruption in 1956, Bezymianny has been active for the past 57 years making it one of the most active volcanoes in Kamchatka (Braitseva et al. 1991, 1995; Plechov et al. 2008). Since the late 1970s, typical activity at Bezymianny consists of dome growth and collapse resulting in block and ash flows, lahars and sub-plinian eruptions with frequencies on the order of one to two eruptions per year (Belousov et al. 1996, 2002). Occasionally, eruptions are followed by short lava flows in the main crater of the volcano.

Klyuchevskoy and Bezymianny share common O, Sr, Pb (not high-precision) and Nd isotopic characteristics, which were interpreted to demonstrate that the two systems originate from a common Klyuchevskoy-type parental magma (Ozerov et al. 1997; Bindeman et al. 2004; Auer et al. 2009, Almeev et al. 2013a). The source of the parental magma is a large melt body imaged geophysically near the Moho (Lees 2007). The current interpretation is that Bezymianny magmas further evolve dominantly through closed-system fractionation in mid-crustal magma chambers (Ozerov et al. 1997; Fedotov et al. 2010; Almeev et al. 2013a; Turner et al. 2013), which may be transient in time (Koulakov et al. 2013) as well as through short-term storage in a

shallow crustal reservoir (Shcherbakov et al. 2011; Turner et al. 2013).

Sample descriptions and petrography

We collected a time-series suite of erupted volcanic products from Bezymianny and Klyuchevskoy volcanoes (sample descriptions in Online Resource 1). Samples were collected during field seasons following observed eruptions (Bezymianny 2006–2010; 1956 lateral blast eruption is easily identifiable) or by collaborators at the Institute of Volcanology and Seismology in Petropavlovsk-Kamchatsky (Klyuchevskoy). Bezymianny samples include five samples from older extrusive domes that surround the modern edifice of the volcano as well as 13 samples from modern eruption products ranging in age from the 1956 directed-blast eruption to the June 1, 2010 pyroclastic flow eruption. Most modern eruptive products from Bezymianny are from bombs with obvious cooling textures (breadcrusted outer surfaces or slumping over larger dense blocks), which were emplaced in pyroclastic flows.

Bezymianny modern eruptive product (1956–2007) textures and mineralogy are described by Plechov et al. (2008), Shipman et al. (2010) and Shcherbakov et al. (2011, 2013). Vesicular andesite is dominated by plagioclase and two-pyroxene phenocrysts. A typical mineral assemblage is plagioclase (modal proportion of up to 70–90 % relative to total phenocrysts), orthopyroxene, clinopyroxene, Fe–Ti oxides and trace apatite and/or amphibole. Orthopyroxene is the dominant pyroxene phase. The groundmass is typically clear glass or glassy with abundant microliters of plagioclase and pyroxene. Plagioclase phenocrysts range in anorthite content from An_{40} to An_{83} and are strongly zoned and have sieve textures. Bezymianny older andesite extrusive domes (56.6–62.8 wt% SiO_2) contain less glass than the modern eruptive products and have abundant large 2–4-mm amphibole phenocrysts in addition to the phases described above. Modern eruptive products do not contain amphibole phenocrysts though amphibole is rarely a trace phase in the microcrystalline groundmass.

The December 2006, October 2007 and August 2008 eruptions at Bezymianny contain enclaves within the sampled juvenile material. Ten enclaves were analyzed in this study. In addition to enclaves, two xenoliths of metamorphosed rock were collected from the October 2007 eruption. Observed enclaves in Bezymianny modern eruptive products have a range of textures but contain mineral assemblages similar to those of the host rocks. Most enclaves have glassy magmatic textures (phenocrysts of plagioclase and pyroxene in a groundmass with Fe–Ti oxides, plagioclase, pyroxene and trace apatite and hornblende). One of the crustal xenoliths, 01BZT09b,
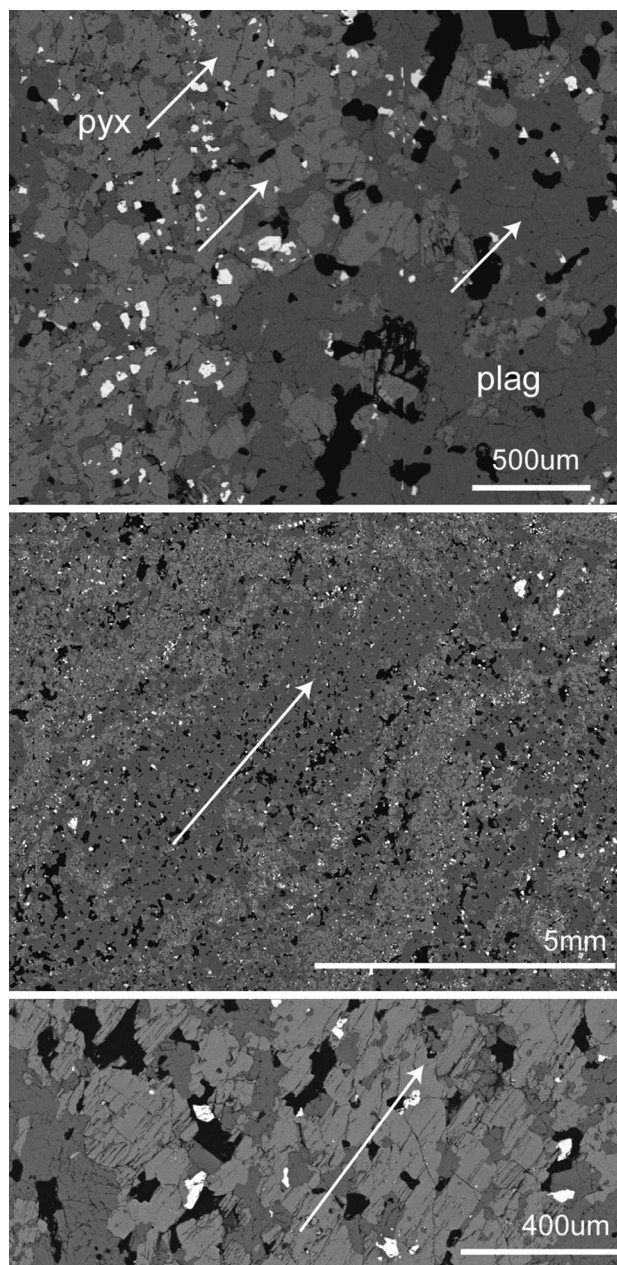
Fig. 2 BSE images of the recrystallized crustal xenolith, 01BZT09b. *Top* BSE image showing recrystallized grains share grain boundaries (*arrows*) at ~120° angles. *Middle* BSE image showing pyroxene (*light gray*) and plagioclase (*dark gray*) minerals are aligned into chains showing minor foliation in the crustal xenolith. *Bottom* BSE image at higher resolution than the middle image showing strain in the individual crystals in the same direction as aligned pyroxene chains

differs dramatically in texture from the enclaves. Sample 01BZT09b has a granular texture indicative of subsolidus recrystallization. Rather than the large plagioclase phenocrysts with complex zoning typical of other Bezymianny samples, this xenolith has small euhedral plagioclase grains that share grain boundaries (Fig. 2). The plagioclase

displays simple twinning and does not display the oscillatory zoning of the magmatic samples. Large pyroxene grains have poikilitic texture enclosing the smaller euhedral plagioclase. These oikocrysts do not consist of just one pyroxene crystal, but are themselves made of many possibly recrystallized clinopyroxene and orthopyroxene crystals that share grain boundaries. The xenolith has an overall minor foliation (aligned chains of pyroxene crystals) as well as abundant Fe–Ti oxides (Fig. 2). Another metamorphic xenolith from the same eruptive unit, 01BZT09c, is similar to 01BZT09b.

Klyuchevskoy samples include five historic lavas erupted between 1945 and 2007. We focused sample collection primarily on the less studied Bezymianny volcano and rely on the wealth of published data from Klyuchevskoy for compositional comparisons and interpretations. The petrography of Klyuchevskoy lavas has been described in detail (Kersting and Arculus 1994; Ariskin et al. 1995; Ozerov et al. 1997; Mironov et al. 2001; Khubanaya et al. 1994; Khubanaya and Sobolev 1998; Auer et al. 2009). Kersting and Arculus (1995) define a complete crystallization sequence from high-magnesian basalts to high-alumina basalts based on mineral compositions and textures. The high-alumina basalts that result from this crystallization sequence have phenocrysts of plagioclase (An_{85-54}), olivine (Fo_{80-85}), augite and orthopyroxene with groundmass plagioclase, olivine, pigeonite and magnetite. Plagioclase and pyroxene phenocrysts have very complex zoning recording multiple recharges of new magma (Kersting and Arculus 1994). One xenolith with cumulate texture was described from Klyuchevskoy deposits as an olivine two-pyroxene gabbro from a 1937 lava flow (K-256, Kersting and Arculus 1994).

We also report new Pb isotope compositions for Shiveluch volcano in the Northern CKD and Karymsky volcano in the Eastern Volcanic Front for comparison to the KG. Sample descriptions for Karymsky and Shiveluch volcano are reported in Online Resource 1.

Analytical methods

Major and trace element analyses

Major and trace element analyses were completed at Washington State University (WSU). Protocols and precision for major element analyses by X-ray fluorescence and trace element analyses by ICP–MS are outlined in Johnson et al. (1999) and in technical notes at the WSU Geoanalytical Laboratory Web site (www.sees.wsu.edu/Geolab/note.html). X-ray fluorescence precision is typically <1 % error for major and minor elements. Long-term precision for ICP–MS is <5 % for REEs and <10 % for all other trace elements.

Pb separation procedure

All samples were cleaned of outer surfaces and rinsed with ultra-clean deionized (DI) H_2O because of the young age of the samples (<60 years for all but the dome samples) samples were not acid-leached prior to analyses. At the time of collection, all samples were isolated from the environment and each other within clean plastic bags. Interior chips were removed from samples and powdered by hand in an agate mortar and pestle that was cleaned between samples by grinding pure silica sand. Approximately 100-mg splits of sample powders were digested in a 10:1 concentrated $HF:HNO_3$ solution on a hot plate at 125 °C. After digestion, samples were dried and re-dissolved in 6 M HCl to convert to Cl^- form and to verify complete dissolution. Samples were dried and brought up in 1 M HBr for ion exchange chromatographic separation of Pb. Lead was purified from the sample matrix using a 300-μl resin bed of BioRad AG-1-X8 100-200 mesh anion exchange resin. The resin is cleaned with 6 M HCl and DI H_2O. Samples are loaded in 1 M HBr, and Pb is eluted with 6 M HCl. The columns are then cleaned, and the separation process is repeated for complete Pb purification. Hydrofluoric acid was suprapure grade (Baseline®) from Seastar, and all other reagents were purified by triple sub-boiling distillation in Teflon. Total procedural blank is less than 50 pg Pb, which is insignificant for the analyzed sample sizes.

Pb isotope MC–ICP–MS analytical procedure

Lead isotope compositions were analyzed by MC–ICP–MS using a Nu Plasma-HR at the University of Washington. Sample introduction was via a Nu Instruments desolvating nebulizer DSN-100 ("dry plasma"). Lead isotope data were collected by static multi-collection that included the measurement of Tl masses (203 and 205) and mass 202 to monitor Hg interference on mass 204. Instrumental mass fractionation was corrected by measuring a Tl spike (SRM 997 thallium isotope standard) and applying an exponential mass fractionation law (Albarède et al. 2004) assuming $^{205}Tl/^{203}Tl = 2.38714$. Thallium spike was added to each sample just prior to analysis (Kamenov et al. 2004) to obtain a Pb/Tl of ~3–4. Mercury interference at mass 204 was subtracted using a natural $^{204}Hg/^{202}Hg$ of 0.229 corrected for instrumental mass fractionation from the Tl measurement. Mercury signal on mass 204 was always less than 0.09 mV and typically less than 0.06 mV. Prior to isotopic analyses, a small aliquot of the sample solution was measured for concentration in order to adjust sample intensity to within 10 % of the intensity of the Pb isotope standard (SRM 981). Samples and standards were run at a concentration of 40 ppb, which yielded 6–8 V of ^{208}Pb signal (with 10^{11} ohm resistors across the faraday cups). The Pb

isotope standard was run after every two samples. The mass fractionation-corrected samples were normalized to bracketing samples as described by White et al. (2000), Blichert-Toft et al. (2003) and Weis et al. (2005) using the SRM 981 isotope ratios determined by double-spike analysis (Todt et al. 1996). Replicate analyses ($n = 19$) of a laboratory internal rock powder standard, UW-BCR-1 (taken from the same location and flow as USGS BCR-1), record 2σ analytical precisions of 150, 225 and 250 ppm for $^{206}Pb/^{204}Pb$, $^{207}Pb/^{204}Pb$ and $^{208}Pb/^{204}Pb$, respectively. Determining reproducibility using duplicate analyses of a rock sample provides a more comprehensive estimate of error as compared to relying on duplicate analyses of a pure Pb isotope standard. Duplicates of 13 different Kamchatka samples were analyzed.

Microprobe analysis

Electron microprobe analyses were performed at the University of Washington using a JOEL 733 SuperProbe equipped with four WDS and one EDS spectrometers. Plagioclase, pyroxene, Fe–Ti oxide, apatite and glass compositions were measured for the 1956 cryptodome (06BZT05), a 2006 breadcrust bomb with clean glass (06BZT02b) and a breadcrust bomb from 2007 with highly microlitic glass (02BZT08). These samples were chosen to represent the spectrum of deposits and textures observed at Bezymianny. In addition to these analyses, plagioclase and pyroxene were measured for the following: an extrusive dome sample from Bezymianny (06BZT08); a basaltic andesite magmatic textured enclave (02BZT09a) from the host 02BZT09b; a mid-crustal xenolith (01BZT09b).

Results

Major and trace element chemistry

Modern Bezymianny compositions range from basaltic andesites to andesites with SiO_2 between 56.6 and 60.2 wt% (Table 1). The older extrusive domes at Bezymianny are slightly more evolved andesites with SiO_2 between 56.6 and 62.8 wt%. While the extrusive domes represent a different eruptive period of Bezymianny prior to the post-1956 activity, they still lie along common chemical trend with the modern eruptive products (Fig. 3). In general, Bezymianny deposits become more mafic with time (Izbekov et al. 2010) as reflected in shifts to lower SiO_2 and higher MgO from the older domes to modern products (Table 1; Fig. 3). Alkali contents ($Na_2O + K_2O$) at Bezymianny are 4.53–4.97 wt% for modern eruptive samples and 4.87–5.48 wt% for the older extrusive domes. Measured Klyuchevskoy lavas have SiO_2 between 53.8

and 54.6 wt%, MgO between 8.3 and 8.5 wt% and alkalis ($Na_2O + K_2O$) between 4.15 and 4.69 wt%. Klyuchevskoy basaltic andesites have higher CaO and TiO_2 and lower Al_2O_3 abundances than modern Bezymianny deposits.

Trace element concentrations of Bezymianny and Klyuchevskoy (Table 1) have typical arc magma characteristics with enrichments in large ion lithophile elements and fluid mobile trace elements and depletions in high-field-strength elements. Incompatible trace element abundances (notably Rb, Ba, Th, U, Pb and La) are slightly higher in the more evolved magmas from Bezymianny than those from Klyuchevskoy. In addition, V and Ti are lower at Bezymianny than Klyuchevskoy consistent with fractionation of Fe–Ti oxides. The Dy/Yb ratios calculated for erupted products are 1.7–1.9 for Bezymianny and 1.9–2 at Klyuchevskoy (Online Resource 2).

Bezymianny mineral chemistry

Plagioclase phenocrysts from Bezymianny volcano range from An_{40} to An_{83} (Online Resource 3) as measured in the older extrusive dome (Lohkmaty), the 1956 cryptodome, and in the modern eruptive products at Bezymianny. Pyroxene phenocrysts at Bezymianny are dominated by orthopyroxene for the older extrusive dome (Lohkmaty), the 1956 cryptodome, and the modern eruptive products. Clinopyroxene is present in these samples, but is much less abundant than orthopyroxene. Orthopyroxene compositions range from ~21–25 wt% MgO and 16–23 wt% FeO with CaO abundances less than 5 wt% (Fig. 4a, b; Online Resource 3). Glass compositions measured for Bezymianny vary depending on whether the glass is clean glass or highly microlitic. Clean glass from 06BZT02b has an average SiO_2 content of 71.0 ± 0.8 wt%.

Bezymianny enclave and xenolith major element and mineral chemistry

Enclaves found in Bezymianny eruptive products are either slightly more mafic (basaltic andesites) than modern Bezymianny magmas (SiO_2 between 53.6 and 57.4 wt%) or overlap in composition with their host magmas (Fig. 3). On the crystal scale, pyroxene compositions measured in the enclave (02BZT09b) are similar to the compositions of pyroxenes from other Bezymianny erupted products and the host magma (02BZT09a; Fig. 4).

The metamorphosed mid-crustal xenoliths (textures described above) from the October 2007 pyroclastic flow of Bezymianny (01BZT09b and 01BZT09c) do not match either Bezymianny or Klyuchevskoy compositions. These xenoliths have mafic compositions (SiO_2 ~51 wt%, MgO ~9 wt%), lower alkali contents ($Na_2O + K_2O$) and higher CaO, MnO and FeO abundances. Rare earth element

Table 1 Major and trace element abundances in Bezymianny and Klyuchevskoy samples

	Bezymianny modern eruptions 1956–present						
Sample name	06BZT02b	06IPE17	02BZT08	06BZT03	06IPE16	06BZT02a	04BZT08
Eruption year	2006	2006	2007	2006	2006	2006	2007
Brief description	Juvenile PF	Juvenile PF	Juvenile PF	Juvenile PF	Juvenile PF	Juvenile PF	Juvenile PF
SiO_2 (wt%)	56.64	57.04	57.12	56.82	56.88	56.85	57.07
TiO_2	0.74	0.76	0.77	0.77	0.76	0.76	0.77
Al_2O_3	18.82	18.34	18.24	18.43	18.38	18.47	18.36
FeO*	6.90	7.03	7.15	7.13	7.14	7.04	6.98
MnO	0.15	0.15	0.15	0.15	0.15	0.15	0.15
MgO	3.82	3.88	3.97	3.98	3.90	3.90	3.94
CaO	7.95	7.64	7.65	7.80	7.69	7.78	7.69
Na_2O	3.51	3.50	3.49	3.46	3.48	3.50	3.48
K_2O	1.07	1.13	1.13	1.09	1.10	1.10	1.12
P_2O_5	0.16	0.17	0.17	0.17	0.16	0.17	0.17
Total	99.76	99.64	99.86	99.81	99.64	99.73	99.73
ICP–MS (ppm)							
La	7.48	7.73	7.96	7.65	7.67	7.78	7.84
Ce	17.34	17.94	18.21	17.77	17.75	17.97	18.00
Pr	2.53	2.62	2.65	2.60	2.60	2.64	2.66
Nd	11.67	11.98	12.11	11.88	11.91	11.97	12.08
Sm	3.05	3.17	3.20	3.16	3.15	3.20	3.20
Eu	1.06	1.07	1.10	1.06	1.06	1.11	1.08
Gd	3.31	3.24	3.50	3.39	3.26	3.31	3.38
Tb	0.55	0.57	0.58	0.57	0.56	0.57	0.57
Dy	3.52	3.64	3.71	3.57	3.47	3.60	3.60
Ho	0.74	0.76	0.77	0.75	0.73	0.76	0.75
Er	2.04	2.08	2.13	2.11	2.04	2.09	2.09
Tm	0.30	0.30	0.31	0.30	0.30	0.30	0.31
Yb	1.90	1.94	1.98	1.96	1.94	1.93	1.99
Lu	0.30	0.31	0.32	0.31	0.31	0.32	0.31
Ba	354	371	371	357	365	364	370
Th	1.03	1.08	1.08	1.03	1.09	1.07	1.06
Nb	1.55	2.02	1.73	1.64	1.85	1.68	1.63
Y	18.44	19.01	19.49	18.95	18.59	19.23	19.14
Hf	2.40	2.54	2.53	2.44	2.43	2.44	2.48
Ta	0.13	0.15	0.15	0.13	0.14	0.13	0.13
U	0.67	0.72	0.72	0.68	0.70	0.70	0.71
Pb	3.50	3.57	3.72	3.51	3.50	3.59	3.62
Rb	18.96	20.22	20.14	19.23	19.89	19.63	19.94
Cs	0.68	0.73	0.76	0.68	0.73	0.71	0.73
Sr	343	333	329	331	338	334	331
Sc	20.25	20.02	22.20	20.02	19.49	19.77	20.98
Zr	87.54	93.11	92.81	89.13	90.10	90.37	91.00
XRF (ppm)							
Ni	10	18	13	12	17	13	12
Cr	17	33	19	19	31	22	22
V	194	194	198	201	198	198	197
Ga	17	17	16	17	17	17	16
Cu	40	34	41	41	39	42	39
Zn	74	77	78	78	78	76	78

Table 1 continued

Sample name	06BZT11	02BZTK07	03BZT08	05BZT08	01BZTK07
Eruption year	1997	2006	2007	1956	2007
Brief description	Juvenile PF	Juvenile PF	Juvenile PF	Juvenile PF	Juvenile PF
SiO_2 (wt%)	56.60	57.36	57.12	60.24	57.08
TiO_2	0.75	0.74	0.77	0.61	0.75
Al_2O_3	18.80	18.50	18.49	18.12	18.47
FeO*	6.92	6.72	6.95	5.83	6.92
MnO	0.15	0.15	0.15	0.15	0.15
MgO	3.88	3.79	3.89	2.68	3.80
CaO	8.00	7.61	7.70	6.71	7.69
Na_2O	3.47	3.54	3.50	3.70	3.53
K_2O	1.06	1.15	1.12	1.27	1.13
P_2O_5	0.17	0.17	0.17	0.18	0.17
Total	99.81	99.73	99.86	99.49	99.69
ICP–MS (ppm)					
La	7.49	8.02	7.93	9.12	7.94
Ce	17.22	18.43	18.18	20.92	18.18
Pr	2.52	2.70	2.69	3.01	2.66
Nd	11.55	12.02	12.14	13.32	11.82
Sm	3.08	3.18	3.18	3.29	3.22
Eu	1.10	1.08	1.08	1.09	1.10
Gd	3.26	3.39	3.37	3.33	3.38
Tb	0.55	0.57	0.58	0.56	0.57
Dy	3.48	3.62	3.67	3.52	3.65
Ho	0.73	0.76	0.76	0.73	0.76
Er	2.04	2.09	2.09	2.06	2.11
Tm	0.29	0.31	0.31	0.30	0.31
Yb	1.85	1.94	1.99	2.01	1.94
Lu	0.31	0.31	0.32	0.33	0.32
Ba	352	377	372	440	374
Th	1.03	1.11	1.11	1.30	1.09
Nb	1.53	1.71	1.70	1.96	1.69
Y	18.53	18.86	19.17	19.14	19.34
Hf	2.35	2.52	2.54	2.86	2.53
Ta	0.13	0.14	0.14	0.16	0.14
U	0.67	0.75	0.74	0.89	0.71
Pb	3.49	3.67	3.75	4.19	3.68
Rb	18.99	20.33	20.16	23.67	20.63
Cs	0.70	0.76	0.72	0.89	0.76
Sr	346	337	337	350	340
Sc	22.42	20.09	20.76	13.74	22.03
Zr	86.59	92.90	92.15	108.56	93.48
XRF (ppm)					
Ni	10	11	11	3	10
Cr	18	18	19	18	19
V	197	186	198	123	191
Ga	17	17	17	17	18
Cu	43	48	35	20	40
Zn	77	76	77	78	76

Table 1 continued

Sample name	Bezymianny enclaves, xenoliths and host juvenile eruptive products						
	01BZT09a	01BZT09b	01BZT09c	02BZT09a	02BZT09b	03BZT09	03BZT09a
Eruption year	2007	2007	2007	2008	2008	2007	2007
Brief description	Enclave	Xenolith	Xenolith	Juvenile host	Enclave	Juvenile host	Xenolith
SiO_2 (wt%)	53.61	50.95	51.06	56.39	53.28	56.67	53.69
TiO_2	0.87	1.02	0.97	0.77	1.00	0.76	1.01
Al_2O_3	18.66	13.06	13.49	18.05	18.17	18.11	17.42
FeO*	8.62	11.06	10.68	7.40	8.85	7.36	7.95
MnO	0.15	0.24	0.23	0.15	0.16	0.15	0.18
MgO	5.07	9.02	8.75	3.98	5.22	3.86	5.27
CaO	8.99	11.76	11.62	7.70	8.79	7.59	8.99
Na_2O	2.89	2.38	2.50	3.44	3.10	3.47	3.96
K_2O	0.77	0.37	0.39	1.08	0.83	1.11	0.68
P_2O_5	0.16	0.33	0.24	0.17	0.16	0.17	0.18
Total	99.80	100.20	99.94	99.13	99.55	99.24	99.34
ICP–MS (ppm)							
La	6.48	3.58	3.24	7.70	6.65	7.86	6.56
Ce	15.38	9.47	8.48	17.91	16.24	18.19	16.29
Pr	2.33	1.58	1.41	2.63	2.52	2.66	2.59
Nd	10.84	8.36	7.44	12.13	11.95	12.12	12.47
Sm	3.07	2.76	2.50	3.18	3.49	3.20	3.60
Eu	1.09	1.05	0.94	1.08	1.14	1.09	1.21
Gd	3.38	3.72	3.30	3.44	3.96	3.43	4.01
Tb	0.58	0.68	0.60	0.58	0.68	0.58	0.68
Dy	3.66	4.46	3.98	3.67	4.35	3.62	4.34
Ho	0.76	0.95	0.84	0.77	0.92	0.75	0.91
Er	2.07	2.61	2.37	2.13	2.52	2.10	2.48
Tm	0.31	0.38	0.34	0.32	0.37	0.32	0.35
Yb	1.92	2.34	2.13	2.00	2.29	2.01	2.19
Lu	0.30	0.36	0.35	0.32	0.36	0.32	0.34
Ba	320	147	155	358	286	367	364
Th	0.79	0.29	0.31	1.03	0.82	1.08	0.81
Nb	1.32	1.16	1.11	1.63	1.58	1.66	1.82
Y	19.30	23.62	20.96	19.69	23.16	19.39	22.66
Hf	2.04	1.52	1.42	2.48	2.41	2.52	2.39
Ta	0.10	0.09	0.08	0.13	0.12	0.14	0.14
U	0.50	0.20	0.20	0.69	0.53	0.71	0.48
Pb	2.88	1.49	1.62	3.60	2.72	3.58	3.25
Rb	14.52	5.85	5.94	19.88	14.85	19.98	12.88
Cs	0.54	0.18	0.19	0.72	0.53	0.73	0.73
Sr	329	195	219	324	281	322	337
Sc	29.13	45.11	42.53	23.04	33.10	22.04	30.58
Zr	73.38	50.19	47.51	91.16	86.93	92.75	88.49
XRF (ppm)							
Ni	21	52	49	14	22	14	25
Cr	18	213	220	18	16	17	67
V	252	358	327	201	280	193	241
Ga	17	16	13	17	16	18	18
Cu	255	91	127	45	128	41	42
Zn	85	111	101	75	74	74	139

Table 1 continued

Sample name	03BZT09b	03BZT09d	04BZT09	04BZT09d	10IPE1A	10IPE1A*	10IPE1B	10IPE1B*
Eruption year	2007	2007	2007	2007	2010	2010	2010	2010
Brief description	Enclave	Enclave	Juvenile host	Enclave	Juvenile host	Enclave	Juvenile host	Enclave
SiO_2 (wt%)	56.63	54.26	56.92	54.36	56.85	57.07	57.38	56.10
TiO_2	0.77	0.89	0.76	0.81	0.80	0.74	0.75	0.80
Al_2O_3	17.38	17.97	18.01	18.67	18.45	18.08	18.21	18.16
FeO*	7.65	8.73	7.28	8.23	8.27	7.20	7.84	7.63
MnO	0.16	0.15	0.15	0.15	0.15	0.15	0.15	0.15
MgO	4.44	4.94	3.89	4.61	4.18	3.78	3.85	4.13
CaO	7.81	8.43	7.54	8.55	8.10	7.61	7.71	7.90
Na_2O	3.25	2.86	3.45	3.04	2.89	3.47	2.97	3.41
K_2O	1.10	0.94	1.13	0.92	1.04	1.12	1.10	1.06
P_2O_5	0.14	0.15	0.17	0.15	0.17	0.18	0.17	0.17
Total	99.33	99.32	99.30	99.51	100.89	99.39	100.12	99.51
ICP–MS (ppm)								
La	7.56	6.99	7.84	7.00	–	7.59	–	7.97
Ce	17.59	16.53	18.31	16.26	–	17.64	–	18.34
Pr	2.65	2.50	2.69	2.44	–	2.63	–	2.68
Nd	12.03	11.61	12.10	11.29	–	12.02	–	12.08
Sm	3.28	3.19	3.17	3.04	–	3.20	–	3.17
Eu	1.07	1.05	1.11	1.10	–	1.10	–	1.07
Gd	3.65	3.53	3.43	3.35	–	3.50	–	3.40
Tb	0.62	0.62	0.57	0.57	–	0.59	–	0.57
Dy	3.94	3.93	3.63	3.58	–	3.72	–	3.63
Ho	0.83	0.83	0.76	0.75	–	0.79	–	0.76
Er	2.29	2.29	2.14	2.10	–	2.15	–	2.08
Tm	0.34	0.34	0.31	0.31	–	0.32	–	0.31
Yb	2.15	2.12	2.00	1.94	–	2.03	–	1.96
Lu	0.35	0.34	0.32	0.32	–	0.32	–	0.32
Ba	356	320	373	360	–	350	–	372
Th	1.07	0.95	1.08	0.85	–	1.00	–	1.09
Nb	1.66	1.55	1.65	1.41	–	1.60	–	1.70
Y	21.31	20.70	19.66	19.11	–	19.89	–	19.44
Hf	2.56	2.45	2.51	2.22	–	2.44	–	2.53
Ta	0.14	0.13	0.14	0.11	–	0.13	–	0.14
U	0.70	0.62	0.72	0.56	–	0.66	–	0.71
Pb	3.70	3.13	3.59	3.71	–	3.38	–	3.61
Rb	20.07	17.10	20.62	17.50	–	19.02	–	20.13
Cs	0.72	0.63	0.72	0.65	–	0.69	–	0.74
Sr	300	297	323	328	–	320	–	325
Sc	27.17	29.44	22.24	25.63	–	23.89	–	21.79
Zr	94.61	88.94	94.13	79.91	–	90.07	–	92.96
XRF (ppm)								
Ni	17	20	13	15	21	12	21	14
Cr	32	16	19	12	19	17	15	16
V	208	253	190	228	202	191	189	211
Ga	16	17	17	18	–	16	–	16
Cu	100	307	41	277	45	36	36	47
Zn	80	77	76	78	82	73	79	77

Table 1 continued

	Bezymianny extrusive domes				
Sample name	06BZT08	06BZT04	06CBZT08	08BZT08	06BZT05
Eruption year	Lokmaty	"youngest"	Cedlo	Expedition	1956
Brief description	Dome	Dome	Dome	Dome	Cryptodome
SiO_2 (wt%)	62.78	61.19	56.62	61.05	60.51
TiO_2	0.51	0.56	0.77	0.60	0.59
Al_2O_3	17.29	17.56	18.76	17.18	17.95
FeO*	4.79	5.15	7.21	5.45	5.83
MnO	0.12	0.13	0.17	0.14	0.15
MgO	2.37	2.71	3.24	2.94	2.60
CaO	5.75	6.24	7.16	6.06	6.53
Na_2O	3.88	3.79	3.77	3.78	3.71
K_2O	1.60	1.48	1.10	1.39	1.29
P_2O_5	0.18	0.18	0.23	0.18	0.18
Total	99.27	98.99	99.03	98.75	99.35
ICP–MS (ppm)					
La	10.85	10.22	9.20	9.82	9.36
Ce	23.73	22.73	21.85	21.87	21.25
Pr	3.30	3.20	3.24	3.08	3.02
Nd	14.02	13.76	15.02	13.42	13.38
Sm	3.20	3.27	3.91	3.23	3.37
Eu	1.02	1.05	1.31	1.05	1.08
Gd	3.08	3.22	4.03	3.20	3.24
Tb	0.51	0.53	0.68	0.52	0.55
Dy	3.20	3.36	4.23	3.28	3.49
Ho	0.66	0.68	0.89	0.67	0.72
Er	1.81	1.93	2.48	1.84	1.98
Tm	0.28	0.29	0.37	0.27	0.30
Yb	1.82	1.85	2.34	1.72	1.91
Lu	0.29	0.31	0.38	0.29	0.32
Ba	602	556	369	496	450
Th	1.63	1.52	0.94	1.38	1.35
Nb	2.14	2.14	2.88	2.15	2.07
Y	17.48	17.99	22.41	17.61	18.79
Hf	3.20	3.07	2.95	3.01	2.91
Ta	0.19	0.18	0.23	0.18	0.16
U	1.12	1.05	0.58	0.91	0.89
Pb	5.42	4.99	2.87	4.79	4.37
Rb	31.41	28.45	18.36	26.50	24.28
Cs	1.12	1.03	0.57	0.94	0.91
Sr	344	358	349	342	350
Sc	11.73	13.06	14.35	15.29	12.50
Zr	125.49	118.18	109.15	111.03	110.41
XRF (ppm)					
Ni	6	11	7	13	6
Cr	28	41	14	62	19
V	98	113	153	119	120
Ga	17	16	18	18	17
Cu	10	6	22	11	18
Zn	69	71	87	76	79

Table 1 continued

	Klyuchevskoy lavas				
Sample name	KL-1939	KL-1945Y	KL-1946A	KL-Krest 07	KL-Aoah 232-07
Eruption year	1939	1945	1946	2007	2007
Brief description	Lava	Lava	Lava	Lava	Lava
SiO_2 (wt%)	53.83	54.14	54.30	54.59	54.28
TiO_2	0.97	1.07	1.07	1.07	1.08
Al_2O_3	16.21	17.96	17.64	17.73	17.60
FeO*	8.29	8.36	8.40	8.45	8.53
MnO	0.17	0.16	0.17	0.18	0.17
MgO	6.89	5.18	5.67	5.21	5.35
CaO	9.23	8.39	8.67	8.54	8.60
Na_2O	3.17	3.55	3.46	3.54	3.48
K_2O	0.98	1.14	1.09	1.04	1.01
P_2O_5	0.19	0.22	0.21	0.20	0.20
Total	99.92	100.15	100.67	100.54	100.30
ICP–MS (ppm)					
La	6.43	7.49	7.29	7.17	7.22
Ce	15.71	18.11	17.63	17.72	17.61
Pr	2.44	2.84	2.72	2.76	2.73
Nd	11.93	13.53	13.25	13.25	13.17
Sm	3.40	3.83	3.69	3.82	3.90
Eu	1.16	1.25	1.27	1.29	1.29
Gd	3.66	4.04	4.00	4.31	4.28
Tb	0.64	0.70	0.70	0.74	0.72
Dy	3.89	4.35	4.37	4.67	4.58
Ho	0.85	0.90	0.88	0.97	0.96
Er	2.28	2.44	2.42	2.68	2.62
Tm	0.33	0.35	0.35	0.38	0.38
Yb	2.07	2.24	2.18	2.39	2.37
Lu	0.32	0.35	0.35	0.37	0.38
Ba	342	391	375	424	420
Th	0.71	0.76	0.78	0.78	0.77
Nb	1.60	1.77	1.77	2.46	1.93
Y	20.92	22.62	22.46	24.51	24.60
Hf	2.29	2.54	2.45	2.63	2.66
Ta	0.11	0.13	0.13	0.15	0.14
U	0.43	0.47	0.46	0.47	0.46
Pb	3.05	3.39	3.20	3.38	3.35
Rb	14.42	16.23	15.46	16.07	15.74
Cs	0.47	0.53	0.48	0.49	0.48
Sr	344	394	378	345	345
Sc	30.80	25.13	28.99	27.85	28.51
Zr	82.06	91.84	90.18	97.06	96.58
XRF (ppm)					
Ni	54	30	33	39	27
Cr	215	42	73	84	65
V	261	263	268	256	260
Ga	16	18	19	18	19
Cu	74	95	97	76	71
Zn	82	86	86	93	90

patterns, normalized to N-MORB, of these samples are flat with normalized REE abundances less than 1.0, unlike other Bezymianny products (Fig. 5). Pyroxene and plagioclase compositions of 01BZT09b differ from the magmatic enclaves and Bezymianny magmas as well. Pyroxenes from this sample have a restricted range in composition relative to other samples. Orthopyroxenes are less Fe rich (~16–19 wt% FeO) and have between ~23 and 26 wt% MgO. Clinopyroxene is more abundant and forms a tight compositional cluster with ~21 wt% CaO, 15 wt% MgO and 8 wt% FeO (Fig. 4a, b). Plagioclase in 01BZT09b also has lower An contents (between An_{40} and An_{62}).

Mineral thermo-barometry

Temperature and pressure of crystallization for the metamorphosed crustal xenolith, 01BZT09b, were calculated using two-pyroxene thermometry and barometry. The orthopyroxene and clinopyroxene in this sample have restricted compositional ranges (Fig. 4a, b), which suggests that the phases reached equilibrium and can be used for P–T determinations. We used the two-pyroxene thermometer and barometer of Putirka (2008) (Eqs. 39 and 37) to calculate pressures and temperatures of pyroxene crystallization for 19 contiguous pairs of clinopyroxene and orthopyroxene (see Appendix C for mineral pair compositions and calculations). In addition to physical proximity, this method requires a test for equilibrium Fe–Mg partitioning between clinopyroxene and orthopyroxene pairs. Equilibrium partitioning between pyroxene grains may be affected by many factors such as Fe^{3+} partitioning (Putirka, pers. comm. 2011). Experiments suggest that equilibrium Fe–Mg exchange should produce $K_D(Fe–Mg)^{cpx-opx} = 1.09 \pm 0.14$ (Putirka 2008). The xenolith pyroxene pairs have $K_D(Fe–Mg)^{cpx-opx} = 0.82 \pm 0.07$, which is within two standard deviations of the experimental equilibrium value. The average calculated temperature and pressure of crystallization from all pyroxene pairs for 01BZT09b are 929 ± 26 °C and 5.2 ± 0.6 kbar or a mid-crustal depth greater than 15 km. This depth calculated from two-pyroxene geobarometry is consistent with a depth of 15 km for magma storage proposed by Almeev et al. (2013b) based on phase equilibria experiments.

Pb Isotope compositions

All samples from Kamchatka have $^{207}Pb/^{204}Pb$ and $^{206}Pb/^{204}Pb$ isotope compositions that plot at or just above the Northern Hemisphere Reference Line (NHRL; Hart 1984) and have MORB-like signatures (Table 2; Fig. 6). We measured Pb isotope compositions for Bezymianny and Klyuchevskoy ($^{208}Pb/^{204}Pb = 37.850–37.903$, $^{207}Pb/^{204}Pb = 15.468–15.480$ and $^{206}Pb/^{204}Pb = 18.249–18.278$ for Bezymianny;

$^{208}Pb/^{204}Pb = 37.907–37.949$, $^{207}Pb/^{204}Pb = 15.478–15.487$ and $^{206}Pb/^{204}Pb = 18.289–18.305$ for Klyuchevskoy) that overlap the unradiogenic extreme of MORB compositions (N-MORB and Pacific MORB) in agreement with the previous studies (Kersting and Arculus 1995; Kepezhinskas et al. 1997; Turner et al. 1998; Churikova et al. 2001).

These high-precision MC–ICP–MS Pb isotope data are the first to reveal that each volcanic center analyzed (Bezymianny, Klyuchevskoy, Shiveluch and Karymsky) is distinct in Pb isotope composition (Fig. 6). Lead isotope compositions for Bezymianny and Klyuchevskoy are less radiogenic than those measured for Shiveluch and Karymsky volcanoes. Bezymianny and Klyuchevskoy compositional distinctions ($^{206}Pb/^{204}Pb$ and $^{208}Pb/^{204}Pb$) occur on very small spatial scales (~9 km). The isotopic contrast between all measured Klyuchevskoy and Bezymianny samples is larger than conservative analytical error (~200 ppm)—with andesitic Bezymianny less radiogenic than its basaltic neighbor, Klyuchevskoy. The Pb isotope compositions of Bezymianny enclaves and xenoliths vary more than individual volcanic centers. Some magmatic enclaves have compositions similar to Bezymianny modern products, while other enclaves and the sampled xenoliths are significantly less radiogenic (Table 2).

Discussion

The magmas at Bezymianny are hypothesized to evolve by fractional crystallization from the parental magmas that feed Klyuchevskoy volcano (Ozerov et al. 1997). While major and trace element data are consistent with this hypothesis, these new Pb isotope data require additional input from an unradiogenic Pb source. Bezymianny products are compositionally more evolved than Klyuchevskoy magmas (Fig. 3), and ratios of incompatible to more compatible trace elements (e.g., Zr/Y, Rb/La, Cs/Yb, Th/Yb and Zr/Sr) increase from Klyuchevskoy to Bezymianny as magmas increase in SiO_2 content (Th/Yb and Zr/Sr shown in Fig. 7). However, Pb isotope data from these volcanoes require that the volcanoes have heterogeneous sources or that crustal assimilation and/or magma mixing occurred during the generation of Bezymianny magmas, mostly in the deeper parts of the system, in order to account for the isotopic contrast between the two volcanic systems. Such assimilation/mixing processes would not significantly alter major and trace element compositions in a manner distinguishable from crystallization of magma during ascent (e.g., Taylor 1980; Reagan et al. 2003), but are uniquely observed in Pb isotope compositions. We develop the hypothesis that deep crustal assimilation and/or magma mixing affects Bezymianny magmas.
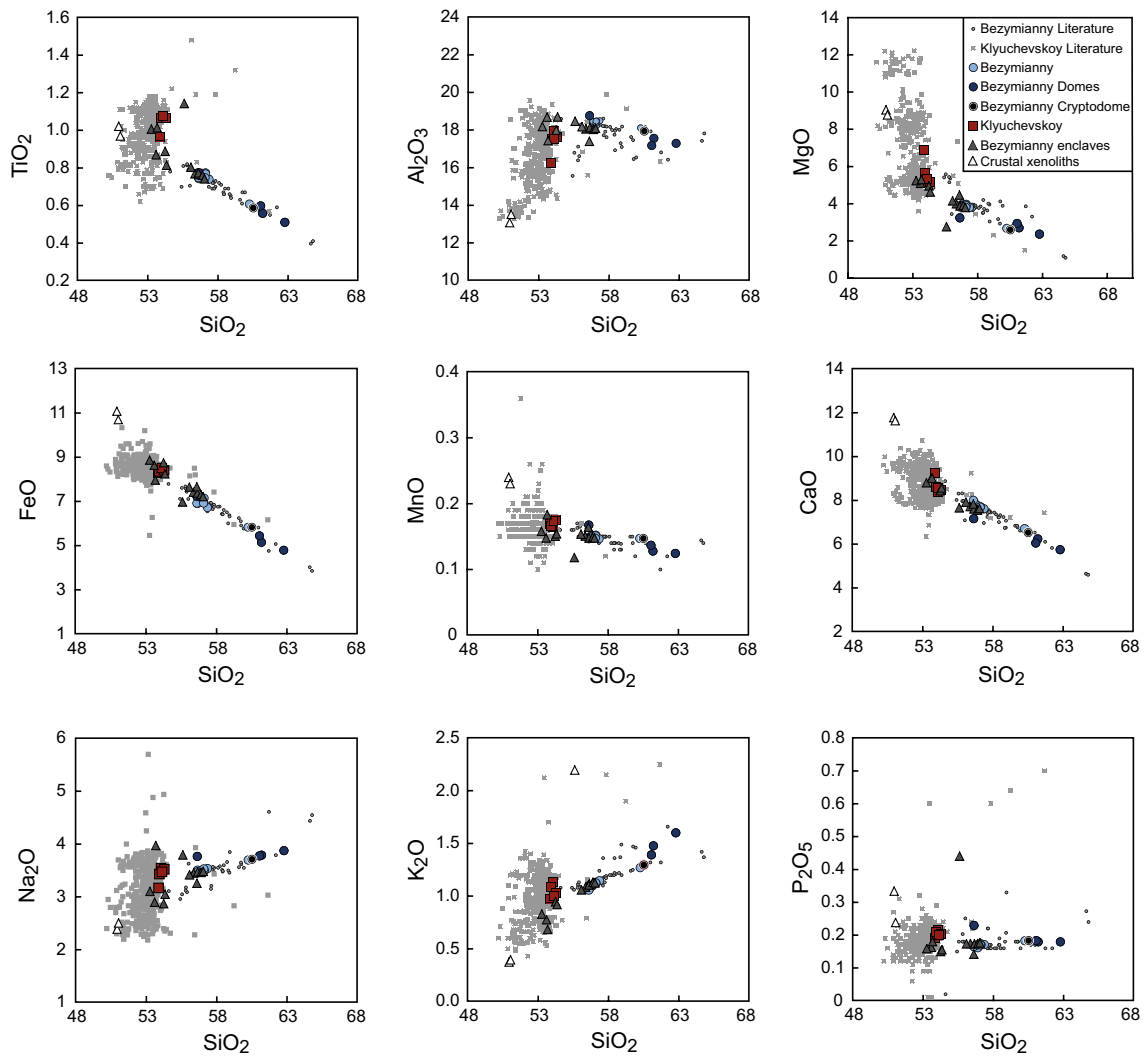
Fig. 3 Harker diagrams for compositions of erupted products from Bezymianny and Klyuchevskoy volcanoes. Bezymianny and Klyuchevskoy data from a review by Portnyagin et al. (2007b) are shown for comparison

Distinct Pb isotope and trace element signatures at Bezymianny and Klyuchevskoy

We resolve a distinctly less radiogenic Pb isotope composition for Bezymianny than for Klyuchevskoy (Fig. 8). The older extrusive domes on the southern edifice of Bezymianny have slightly more radiogenic Pb than the modern eruptions of Bezymianny and trend toward Klyuchevskoy compositions (Fig. 8). However, even these more radiogenic extrusive dome compositions do not overlap Klyuchevskoy compositions. To ensure that distinct Pb isotope compositions at Bezymianny do not result from the investigation of only five Klyuchevskoy lavas, these data are compared with published Klyuchevskoy data. Klyuchevskoy data presented here compare well with the published Pb isotope data (Portnyagin et al. 2007b) (Fig. 8) and are similar to unpublished, high-precision double-spike Pb isotope data for 25 Klyuchevskoy

tephras that span 6,000 years of eruptive activity from ^{14}C age 200BP to 6800 BP (Portnyagin, pers. comm. 2012; Portnyagin et al. 2011; Portnyagin and Ponomareva 2012). The large Klyuchevskoy dataset overlaps only the older Bezymianny compositions and is entirely more radiogenic than 1956–recent Bezymianny products. Therefore, we interpret the contrast in Klyuchevskoy and Bezymianny Pb isotopes to be real rather than a result of sampling bias.

If Bezymianny magmas were the product of closed-system fractionation of Klyuchevskoy magma in an upper crustal magma chamber (Ozerov et al. 1997), then the Pb isotope composition of Bezymianny products should be the same as Klyuchevskoy. Including assimilation of *upper* crust in the Ozerov et al.'s (1997) fractional crystallization model would not explain the less radiogenic Pb isotope composition of Bezymianny. The absence of substantial intracrustal differentiation and the young age of crust
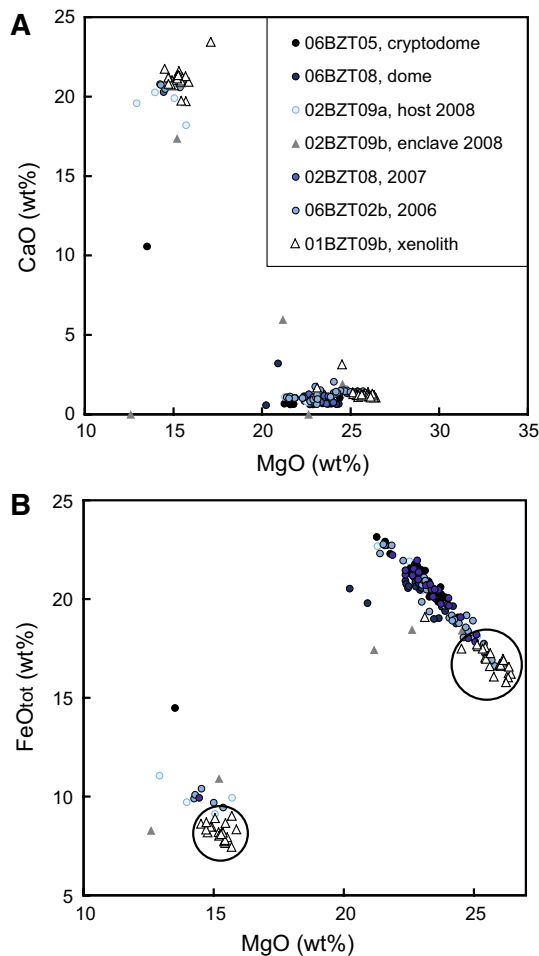
Fig. 4 Clinopyroxene and orthopyroxene compositions from Bezymianny erupted products. **a** The majority of pyroxenes from the extrusive domes, the 1956, 2006 and 2007 eruptions, as well as from the enclaves are orthopyroxenes with similar compositions (20–25 wt% MgO). **b** *Circles* highlight pyroxene compositions for the mid-to-lower crustal xenolith relative to compositions from other eruptions. Compositions of pyroxenes from the lower crustal xenolith (01BZT09b) differ from typical Bezymianny pyroxene compositions (*white triangles* in **a** and **b**). Clinopyroxene and orthopyroxene from the xenolith form two tight clusters in compositional space in contrast to the broader range recorded in other Bezymianny juvenile products

Fig. 5 Rare earth element patterns for Bezymianny and Klycuhevskoy erupted products normalized to N-MORB (Hofmann 1988). Bezymianny domes, juvenile samples from 1956 to 2007 and enclaves all have enriched LREE and depleted HREE relative to N-MORB. The extrusive domes are slightly more enriched in LREEs than the modern eruptions (shown in *left inset*). Bezymianny erupted products and extrusive domes have enriched light REEs and depleted mid-to-heavy REEs relative to Klyuchevskoy lavas (shown by crossing pattern of Klyuchevskoy lavas over Bezymianny compositions in *right inset*). Most enclaves from Bezymianny have REE compositions that overlap modern Bezymianny products (*stipled shaded* region on graph). However, two crustal xenoliths, 01BZT09b and 01BZT09c, found in bombs from the October 2007 eruption have flat to depleted REE patterns relative to N-MORB (*dotted lines*). 01BZT09b is the xenolith inferred through thermobarometry to be a mid-to-lower crustal inclusion

in Kamchatka (Cenozoic: Fedotov et al. 1991; Dorendorf et al. 2000) make developing any contrast in Pb isotope composition between upper crust and erupted products by radiogenic ingrowth unlikely. Further, if a Pb isotope contrast does develop with aging of the upper crust, it would be toward relatively more radiogenic Pb, not the relatively less radiogenic Pb observed in Bezymianny. In addition, many trace element ratios of samples from Bezymianny have trends that parallel with those of Klyuchevskoy but are offset in Pb isotope composition (Fig. 7). For example, Zr/Sr and Th/Yb both increase with magmatic differentiation and positively correlate with $^{206}Pb/^{204}Pb$. Therefore, magmas

beneath Bezymianny and Klyuchevskoy may evolve in the upper crust in a similar fashion toward higher incompatible element concentrations and more radiogenic Pb, but they likely evolve from distinct deeper magma sources with different isotopic compositions. Indeed, time-dependent seismic tomography resolves a short-lived direct melt channel from the mantle to Bezymianny in 2005 that is separated from the crustal magma reservoirs of Klyuchevskoy (Koulakov et al. 2013). These observations suggest that the Bezymianny magma system includes melt with a Pb isotope composition that cannot be sourced from Klyuchevskoy without significant modifications.

Enclaves and xenoliths from Bezymianny modern eruptive products also have Pb isotope compositions that are distinct from Klyuchevskoy. Most of the sampled enclaves have Pb isotope compositions matching the modern eruptive products at Bezymianny and are likely cogenetic with their host eruptive units (Fig. 8). However, two xenoliths and two enclaves have lower $^{207}Pb/^{204}Pb$ and $^{206}Pb/^{204}Pb$ than modern Bezymianny magmas (01BZT09b, 01BZT09c, 02BZT09b and 10IPE1B from the October 2007, August 2008 and June 2010 eruptions).

Table 2 High-precision MC–ICP–MS Pb isotope compositions

Sample name	Eruption date	$^{208}Pb/^{204}Pb$	$^{207}Pb/^{204}Pb$	$^{206}Pb/^{204}Pb$	n[a]	Description
Bezymianny Volcano						
Bezymianny extrusive domes						
06BZT04	<3 ka	37.903	15.478	18.277		"Young" dome
06BZT08	3–5 ka	37.899	15.478	18.276		Lokmaty dome
08BZT08[b]	Holocene	37.903	15.478	18.278	3	Expedition dome
06CBZT08	Pleistocene	37.870	15.473	18.268		Cedlo dome
MP1BZT09	Unknown	37.865	15.471	18.262		Mega plag lava
MP2BZT09	Unknown	37.881	15.475	18.269		Mega plag lava
Bezymianny modern eruptions 1956–present						
06BZT05	1956	37.889	15.474	18.259		Cryptodome
05BZT08	1956	37.886	15.475	18.262		Cryptodome
06BZT11	1997	37.889	15.477	18.262		Pumice, tephra
06IPE16	2006 (May)	37.878	15.474	18.255		Juvenile breadcrust bomb
06IPE17	2006 (May)	37.875	15.471	18.256		Juvenile breadcrust bomb
06BZT02a	2006 (May)	37.872	15.471	18.255		Juvenile breadcrust bomb
06BZT02b[b]	2006 (May)	37.879	15.474	18.256	2	Inner, breadcrust bomb
06BZT03	2006 (May)	37.867	15.471	18.257	2	Pumice
02BZTK07	2006 (Dec)	37.882	15.474	18.260		Juvenile breadcrust bomb
05BZT09[b]	2006/2007	37.882	15.474	18.261	2	Juvenile breadcrust bomb
01BZTK07	2007 (May)	37.892	15.478	18.262		Juvenile breadcrust bomb
02BZT08	2007 (Oct)	37.881	15.475	18.260		Juvenile breadcrust bomb
03BZT08	2007 (Oct)	37.877	15.474	18.249		Juvenile breadcrust bomb
04BZT08	2007 (Oct)	37.882	15.475	18.260		Juvenile breadcrust bomb
03BZT09	2007 (Oct)	37.888	15.475	18.265		Juvenile breadcrust bomb
04BZT09	2007 (Oct)	37.896	15.480	18.266		Juvenile breadcrust bomb
11BZT09	2007 (Oct)	37.888	15.477	18.262		Juvenile breadcrust bomb
06BZT09	2008 (Aug)	37.890	15.477	18.269		Juvenile bomb
10IPE5A	2009 (Dec)	37.889	15.479	18.260		Juvenile breadcrust bomb
10IPE7A	2009 (Dec)	37.893	15.479	18.261		Juvenile breadcrust bomb
10IPE8	2010 (Jan/Feb)	37.892	15.480	18.259		Lava flow
10IPE1A	2010 (June)	37.886	15.476	18.268		Juvenile bomb
10IPE2A	2010 (June)	37.892	15.478	18.265		Juvenile bomb
10IPE9	2010 (June)	37.893	15.479	18.257		Lava flow
Bezymianny enclaves and xenoliths						
01BZT09a	2007 (Oct)	37.881	15.475	18.259		Enclave in 02BZT08
01BZT09b[b]	2007 (Oct)	37.828	15.473	18.183	3	Xenolith in 02BZT08
01BZT09c	2007 (Oct)	37.854	15.473	18.231		Xenolith in 02BZT08
03BZT09a	2007 (Oct)	37.893	15.476	18.276		Xenolith in 03BZT09
03BZT09b	2007 (Oct)	37.890	15.476	18.267		Enclave in 03BZT09
03BZT09d	2007 (Oct)	37.892	15.478	18.264		Enclave in 03BZT09
04BZT09d	2007 (Oct)	37.892	15.476	18.265		Enclave in 04BZT09
11BZT09a	2007 (Oct)	37.873	15.471	18.261		Enclave in 11BZT09
05BZT09a[b]	2006/2007	37.889	15.477	18.263	2	Enclave in 05BZT09
05BZT09b[b]	2006/2007	37.893	15.477	18.268	2	Enclave in 05BZT09
02BZT09b[b]	2008 (Aug)	37.815	15.472	18.200	3	Enclave in juvenile bomb
06BZT09a	2008 (Aug)	37.883	15.473	18.263		Enclave in 06BZT09
10IPE5B	2009 (Dec)	37.886	15.476	18.257		Enclave in 10IPE5A
10IPE7B	2009 (Dec)	37.897	15.481	18.256		Enclave in 10IPE7A

Table 2 continued

Sample name	Eruption date	$^{208}Pb/^{204}Pb$	$^{207}Pb/^{204}Pb$	$^{206}Pb/^{204}Pb$	n[a]	Description
10IPE1B[b]	2010 (June)	37.800	15.477	18.166	3	Enclave in 10IPE1A
10IPE2B	2010 (June)	37.880	15.477	18.252		Enclave in 10IPE2A
Klyuchevskoy Volcano						
Klyuchevskoy lavas						
KL 1939	1939	37.915	15.480	18.291		Lava flow, flank
KL 1945Y	1945	37.907	15.478	18.289		Lava flow, flank
KL 1946A	1946	37.918	15.483	18.294		Lava flow, flank
KL Krest07	2007	37.949	15.487	18.305		Lava flow, summit
KL-Apah 232-07	2007	37.944	15.484	18.303		Lava flow, summit
Shiveluch Volcano						
Shiveluch modern eruptions 1964–2007						
SHIV 1964	1964	37.912	15.483	18.361		Juvenile clast, pyroclastic flow
SHIV 1980[b]	1980	37.934	15.487	18.378	2	Juvenile clast, pyroclastic flow
SHIV 1993	1993	37.910	15.483	18.364		Juvenile clast, pyroclastic flow
SHIV2001 PFDMB	2001	37.901	15.479	18.362		Juvenile clast, pyroclastic flow
SHIV2001DMB[b]	2001	37.875	15.476	18.312	2	Dome
SHIV7 2007	2007	37.908	15.483	18.357		Juvenile clast, pyroclastic flow
Karymsky Volcano						
Karymsky modern eruptions 1971–2007						
KTK0308	1964	37.988	15.484	18.360		Lava flow
K1971 PFMB	1971	37.994	15.487	18.362		Juvenile bomb, pyroclastic flow
KTK0408	1971	37.993	15.485	18.362		Lava flow toe
97IPE4[b]	1996 (Apr–Aug)	37.998	15.488	18.363	3	Lava flow
98IPE28	1996 (Sep–Oct)	37.983	15.483	18.360		Lava flow
98IPE22d[b]	1996	37.980	15.482	18.360	2	Juvenile bomb, Academy Nauk
98IPE26	1998 (June–July)	37.994	15.487	18.363		Lava flow
K2003	2003	37.985	15.483	18.359		Lava flow
K2004	2004	37.983	15.483	18.359		Lava flow
K2007[b]	2007	37.992	15.490	18.345	2	Ash, collected while falling
KTK0508	2008 (April)	38.001	15.489	18.366		Juvenile bomb
KTK0908	2008 (July 25)	38.002	15.489	18.366		Juvenile bomb

[a] Number of duplicates used to produce average value reported

[b] The value reported results from the averaging of multiple duplicate analyses

Origin of isotopic and chemical contrasts between Bezymianny and Klyuchevskoy

We evaluate three hypotheses to explain the chemical and isotopic contrast between Bezymianny and Klyuchevskoy: (1) Klyuchevskoy magmas may assimilate more radiogenic material on their path through the crust to shift them to higher $^{207}Pb/^{204}Pb$ and $^{206}Pb/^{204}Pb$ than measured at Bezymianny, (2) Sediment contamination in the source of Klyuchevskoy that is absent in the Bezymianny source produces more radiogenic Pb isotope signatures at Klyuchevskoy and (3) there may be multiple magma sources or crustal contaminants beneath Bezymianny and Klyuchevskoy that are recorded by the lower $^{207}Pb/^{204}Pb$ and $^{206}Pb/^{204}Pb$ of the Bezymianny enclaves and xenoliths.

Hypothesis 1: Klyuchevskoy Magmas Assimilate Material with a Radiogenic Pb Isotope Signature.

If Bezymianny and Klyuchevskoy share magmas in a deep chamber, then Klyuchevskoy must acquire more radiogenic Pb than Bezymianny at shallower levels. Typically, upper crust is more radiogenic than lower crust as a function of differentiation and age of continental/island arc crust (Hofmann 1997). Due to the juvenile nature of the Kamchatka arc, however, there is no geochemical rationale to postulate the presence of a significantly more radiogenic upper crust. Geochemical constraints such as the high Mg# of Klyuchevskoy magmas, low SiO_2 contents and MORB-like Nd and Sr isotope compositions (Kersting and Arculus 1995; Dorendorf et al. 2000; Portnyagin et al. 2007b)
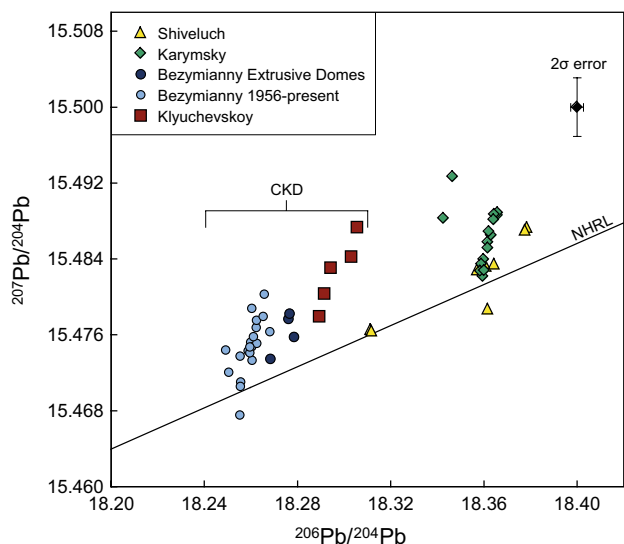
Fig. 6 Pb isotope compositions from Kamchatka by high-precision MC–ICP–MS analyses. Two-sigma analytical error of 150 ppm (^{206}Pb/^{204}Pb) and 225 ppm (^{207}Pb/^{204}Pb) resolves isotopic differences between Bezymianny, Klyuchevskoy, Shiveluch and Karymsky volcanic centers. Pb isotope compositions in the Central Kamchatka Depression (CKD) are less radiogenic than those from the Eastern Volcanic Front (Karymsky) and Northern CKD (Shiveluch). NHRL (Northern Hemisphere Reference Line) from Hart (1984)

Fig. 7 Parallel differentiation patterns of Bezymianny and Klyuchevskoy erupted products. Both Zr/Sr and Th/Yb positively correlate with ^{206}Pb/^{204}Pb at each volcanic center. Patterns suggest that the magmas of these neighboring volcanoes may evolve in a similar way to higher incompatible element concentrations and more radiogenic Pb within the upper crust beneath the CKD. The distinct ^{206}Pb/^{204}Pb between the two volcanic centers requires heterogeneous deep magma sources, magma mixing or assimilation

make upper crustal assimilation unlikely at Klyuchevskoy. MORB-like Nd isotope compositions coupled with slightly radiogenic Sr isotopes are not consistent with assimilation of old crustal terranes and suggest that if assimilation occurs, magmas would assimilate juvenile crust with isotopic compositions similar to MORB (Kersting and Arculus 1995). Dy/Yb ratios are consistent between the two volcanic systems and invariant with SiO_2 (Online Resource 4), so it is unlikely that amphibole fractionation or assimilation in the upper crust results in compositional variation; otherwise, Dy/Yb ratios would vary between volcanoes (Davidson et al. 2007).

In addition, assimilation of the upper crust within the Klyuchevskoy magmatic plumbing system is unlikely from geophysical and thermal modeling perspectives. Reconstruction of the volcanic structure of Klyuchevskoy based on geophysical data suggests that magma moves from the mantle and/or base of the crust to the surface through a narrow vertical conduit that lacks crustal magma chambers (Anosov et al. 1978; Ozerov et al. 1997, 2007; Lees et al. 2007). An earthquake catalog and geodetic measurements show evidence for a shallow magma body approximately 3 km beneath Klyuchevskoy (Fedotov et al. 2010). However, this shallow magma is located in "sedimentary" layers of young volcanic material (Fedotov et al. 2010), which would not have a significant Pb isotope contrast from current eruptive products in the KG.

Assimilation of upper crustal material likely is also thermally inhibited (Dufek and Bergantz 2005) and causes crystallization and evolution of magmas (Reiners et al. 1995) that is not reflected in Klyuchevskoy lavas. Therefore, the hypothesis that a common parental Klyuchevskoy–Bezymianny magma has a modified Pb isotope composition due to assimilation of radiogenic crust in Klyuchevskoy is not consistent with the geophysical evidence or geochemical compositions of Klyuchevskoy.

Hypothesis 2: Subducted Sediment Alters Magmatic Pb Isotope Composition.

Previous models based on isotope systematics coupled with major element trends at Klyuchevskoy and within the CKD constrain the amount of sediment that was added to the mantle source via subduction (Kersting and
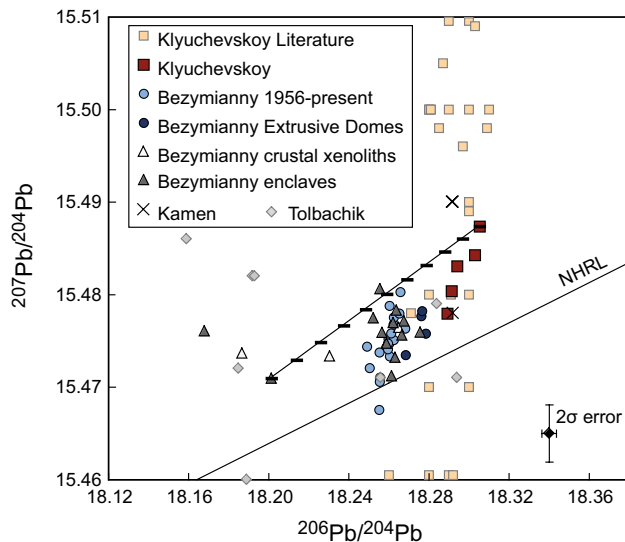
Fig. 8 Pb isotope compositions of Klyuchevskoy group magmas relative to the Northern Hemisphere Reference Line (NHRL). Bezymianny and Klyuchevskoy compositions are represented using symbols from Fig. 7. Bezymianny enclaves are shown as *gray triangles*, and crustal xenoliths are shown as *white triangles*. Most enclaves have similar compositions to Bezymianny juvenile products; however, two enclaves and two xenoliths are less radiogenic (samples 01BZT09b, 01BZT09c, 02BZT09b and 10IPE1B). Klyuchevskoy literature data are shown as *small squares* relative to Klyuchevskoy lavas from this study and Bezymianny compositions. All Klyuchevskoy products are more radiogenic than modern Bezymianny erupted products. Klyuchevskoy literature data have order of magnitude larger errors (not shown) from TIMS analysis. Lead isotope compositions of other CKD volcanic centers located near Bezymianny are also shown (Kamen *crosses*; Tolbachik *gray diamonds*). Published Pb isotope compositions for Tolbachik volcano are less radiogenic than Bezymianny modern erupted products and plot near the compositions of the Bezymianny enclaves. Compositions for Kamen volcano are similar to Klyuchevskoy and more radiogenic than Bezymianny. A magma mixing curve is shown between a Klyuchevskoy lava and a basaltic andesite enclave (black line, tick marks represent 10 % mixing intervals). The composition of Bezymianny can be explained by ~40–60 % mixing of an enclave composition with a Klyuchevskoy magma composition. Literature data shown are from a compilation of Portnyagin et al. (2007b) and Churikova et al. (2001)

Arculus 1995; Kepezhinskas et al. 1997; Dorendorf et al. 2000; Churikova et al. 2001). If Pb isotope compositions of sediments from the ODP Leg 145 drilling in the northwest Pacific Ocean (drilled parallel to the Kamchatka Arc approximately 450 km east of the trench) are characteristic of sediment subducted beneath the arc, Kersting and Arculus (1995) show that the amount of sediment input to the Kamchatka mantle source must be less than 1 % in order to preserve the MORB isotopic compositions in erupted products. Tsvetkov et al. (1989) came to a similar conclusion based on Be isotopes. Dorendorf et al. (2000) interpreted Sr and O isotopes to show that fluids come from the altered oceanic crust and not subducted sediments. While in general, sediment addition to the source is limited, we refine

this model specifically for Bezymianny and Klyuchevskoy using new high-precision Pb isotope data. We also note that other segments of the Kamchatka arc, such as the Eastern Volcanic Front, may show evidence for sediment addition from the subducted slab (Duggen et al. 2007), and therefore, the modeling for this study only applies to the Klyuchevskoy Group of the Central Kamchatka Depression.

We use an average ODP 145 drill core sediment composition (Kersting and Arculus 1995) of $^{207}Pb/^{204}Pb = 15.6$, $^{206}Pb/^{204}Pb = 18.6$ and [Pb] = 11.5 ppm. Mixing calculations with the lowest range of N-MORB Pb isotope compositions (Hofmann 1988; Sun and McDonough 1989) allow 0 % of sediment to be added to the mantle wedge because $^{207}Pb/^{204}Pb$ and $^{206}Pb/^{204}Pb$ values at Bezymianny and Klyuchevskoy are less radiogenic than N-MORB. If an average Pacific MORB mantle composition is used, the same conclusion is drawn. The only scenario by which sediment may be added to the mantle wedge is whether the wedge is assumed to have the least radiogenic Pacific MORB values reported. We assume a Pacific MORB composition, that is, two standard deviations below the mean for Pacific MORB (Arevalo and McDonough 2010), so as to represent a "low" Pacific MORB value, but one that is not the lowest singular measured value. With a mantle wedge of this composition, 0.2 and 0.4 % sediment at Bezymianny and Klyuchevskoy, respectively, can be accommodated if sediment is added to a fluid-fluxed solid mantle that has a Pb concentration of 0.16 ppm (Fig. 9a). Kersting and Arculus (1995) calculated a Pb concentration of the fluid-fluxed solid mantle beneath Klyuchevskoy of 0.16 ppm by taking a mantle composition of 0.031 ppm (Stolper and Newman 1994; note this value is similar to the Salters and Stracke (2004) depleted mantle Pb concentration of 0.023 ppm) and fluxing the mantle with Pb-rich fluid at a porosity of 1 % to create a composition of 0.16 ppm. If sediment is added to a fluid-fluxed mantle *melt* of this depleted source (melt Pb concentration now increased to 3 ppm) rather than to a solid mantle source, then 4 and 7 % sediment may be added to Bezymianny and Klyuchevskoy sources, respectively (Fig. 9b). Because this calculation relies on the choice of an extreme Pacific MORB end-member, this represents a maximum amount of possible sediment addition.

Measured Ce/Pb ratios are approximately the same for Klyuchevskoy (5.15–5.52) and modern Bezymianny (4.38–5.07; Fig. 10). These values are within the range of typical arc basalts (1–10: Miller et al. 1994; Noll et al. 1996; Plank 2005) and are low compared to MORB values (Hofmann 1988). The lower Ce/Pb ratios of arc basalts reflect addition of a slab fluid (Brenan et al. 1994; Miller et al. 1994), or partial melt of the subducting slab or sediment (Tatsumi 2000; Kelemen et al. 2003). If sediment contamination affected the Pb isotope compositions at Bezymianny and Klyuchevskoy, it should impart a high $^{207}Pb/^{204}Pb$ and

^{206}Pb/^{204}Pb signal coupled with a low Ce/Pb ratio. However, Klyuchevskoy has equal or higher Ce/Pb relative to Bezymianny. These observations extend to the published dataset for Klyuchevskoy (Portnyagin et al. 2007b, which includes a compilation of previously published Pb isotope data). Coupling Ce/Pb evidence with the sediment modeling suggests that it is unlikely the measured Pb isotope variations between Bezymianny and Klyuchevskoy are a result of variable sediment contamination of the mantle source region. Because the Ce/Pb ratios between Bezymianny and Klyuchevskoy are similar, it is also unlikely that the variation in the Pb isotopes may be explained by an increased slab fluid component in the mantle source for Bezymianny magmas.

Hypothesis 3: Multiple Magma Sources or Contaminants Beneath Bezymianny Volcano—Part 1: Mantle or Slab Heterogeneities.

In any arc magmatic system, it is possible that small-scale mantle heterogeneities and/or slab heterogeneities exist, inducing Pb isotope variation in magmas. Small-scale (<10s of kilometers) mantle heterogeneity has been documented in volcanoes associated with mantle plumes (Abouchami et al. 2005; Brunelli and Seyler 2010; Madureira et al. 2011). Variation in the Pb isotope signature of the KG may solely reflect a heterogeneous mantle source that varies in composition on a small spatial scale. The presence of the Emperor seamount chain on the subducting plate in the North Pacific may affect the mantle source and modify the Pb isotope composition within the KG. For example, Meiji seamount (85 Ma) off the coast of Kamchatka is less radiogenic in both ^{207}Pb/^{204}Pb and ^{206}Pb/^{204}Pb than Bezymianny and Klyuchevskoy magmas (Regelous et al. 2003). In addition, Pb isotope heterogeneity from 18.25 to 18.70 in the ^{206}Pb/^{204}Pb ratio occurs on spatial scales as small as one lava eruption (Abouchami et al. 2005). It is difficult to make an analogy between processes that preserve small-scale mantle heterogeneity measured in Hawaiian lavas and the Emperor seamount chain with processes in the volcanic arc environment. Rather than preserving mantle heterogeneity through thin oceanic crust, the arc environment requires geochemical preservation of chemical heterogeneity during transport through the mantle wedge, the crust and within crustal magma reservoirs. Models that support melt channeling (Spiegelman and Kelemen 2003) address the complexity of this issue and show that even a single magma can undergo physical melt channeling resulting in orders of magnitude differences in trace element compositions. We cannot rule out the presence of small-scale heterogeneities in the mantle/slab beneath KG. However, to create the Pb isotope contrast between Bezymianny and Klyuchevskoy through preserving small-scale (~km)

mantle heterogeneities would require that inherited heterogeneity survived melt transport through the mantle, crust and possible magma pooling at the lower crust interface, as inferred from geophysical data (see below).

Hypothesis 3: Part 2: Magma Mixing at Bezymianny.

Because two enclaves and two crustal xenoliths found in Bezymianny eruptive products have relatively unradiogenic Pb compositions, we investigate the possibility that magma mixing and assimilation and fractional crystallization may explain the magma compositions at Bezymianny. The enclaves have magmatic textures with mineral assemblages similar to their hosts and may, therefore, represent residues of magmas that mixed with Bezymianny magmas. The two xenoliths are fragments of mid-crustal lithologies, which may represent material that Bezymianny magma assimilates during residence in the crust. Magma mixing and deep crustal reservoirs beneath Bezymianny are supported by recent inferences from petrology, geochemistry, gas chemistry and tomography (Almeev et al. 2013a; Koulakov et al. 2013; Lopez et al. 2013; Turner et al. 2013).

Basaltic andesite enclaves, such as 02BZT09b, may serve as a hypothetical magma end-member to model mixing with Klyuchevskoy magmas (KL-Krest-07) to produce the lower Pb isotope compositions of Bezymianny. Using the Pb isotope compositions and Pb concentrations for these two samples and simple two-component mixing, Bezymianny compositions would be produced by 40–60 % mixing of magma with the enclave composition into Klyuchevskoy-like magmas (Fig. 8). An influx of a less differentiated magma to the Bezymianny magma system would explain the more mafic composition of Bezymianny inclusions compared to the modern eruptive products (Fig. 3).

Magmas from Tolbachik and Kamen volcanoes (Fig. 8) represent other possible magma mixing end-members beneath Bezymianny. The Pb isotope compositions of magmas from both the primary edifice of Tolbachik and the 1975 great fissure eruption of Tolbachik are low relative to Bezymianny and overlap with Bezymianny inclusion compositions. Although the edifice of Tolbachik volcano is 20 km southwest of Bezymianny volcano, a linear trend of volcanic cones and domes between the two volcanoes (Online Resource 2) may reflect a structure in the crust along which mafic magma from Tolbachik could interact with Bezymianny magmas. In addition, Bezymianny trace element trends show a shift in the mid-1970s (Izbekov et al. 2010; Turner et al. 2013) that could correlate with the timing of the Tolbachik great fissure eruption and may explain some of the mafic input at Bezymianny volcano. Churikova et al. (2011) suggest that Kamen and Bezymianny share similar sources; however, published Pb isotope data from Kamen have Klyuchevskoy-like compositions rather than
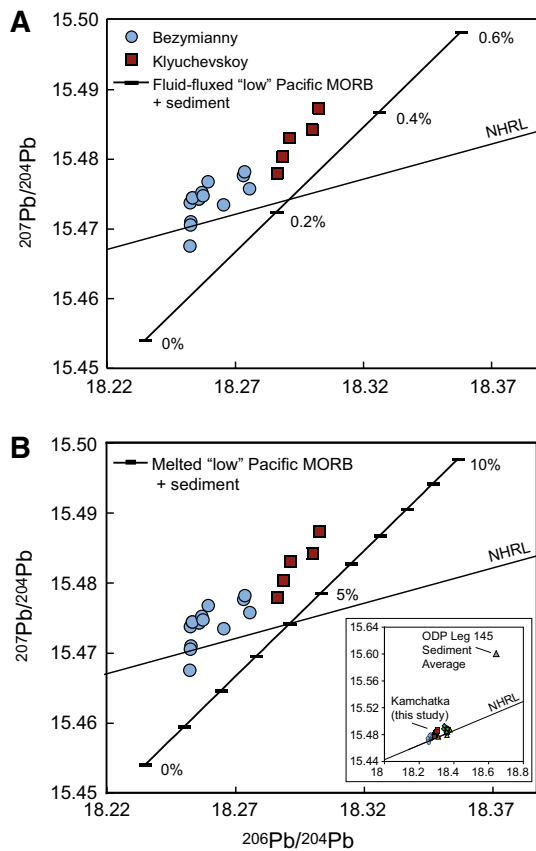
Fig. 9 Sediment mixing models for the Central Kamchatka Depression. **a** Mixing curve shows addition of sediment to a fluid-fluxed solid mantle (composition described in text). *Tick marks* represent 0.2 % intervals of mixing. Sediment composition is an average for sediments off the coast of Kamchatka (ODP Leg 145, Kersting and Arculus 1995). The initial composition of the mantle is a value two standard deviations less radiogenic than the mean for Pacific MORB (Arevalo and McDonough 2010)—referred to here as a "low" Pacific MORB. Concentration of Pb in the mantle is 0.16 ppm (Kersting and Arculus 1995) and represents a mantle composition (Pb = 0.031 ppm) with fluid added from the slab at 1 % porosity to create the 0.16 ppm Pb concentration. Bezymianny and Klyuchevskoy compositions can be generated with 0.2–0.4 % sediment added to a mantle source. **b** Mixing curve showing the addition of sediment (described for **a**) to a fluid-fluxed mantle *melt*. Concentration of Pb is 3 ppm in the melt from the mantle. *Tick marks* denote 1 % intervals of sediment mixing. This model allows for more sediment addition (4–7 %)

the less radiogenic compositions of Bezymianny (Fig. 8), so Kamen compositions likely do not contribute to Bezymianny magmas.

Hypothesis 3: Part 3: Lower-Crustal Assimilation Beneath Bezymianny.

The presence of two mid-crustal xenoliths (01BZT09b and 01BZT09c) within Bezymianny samples lends support to the hypothesis of middle or lower-crustal assimilation, a
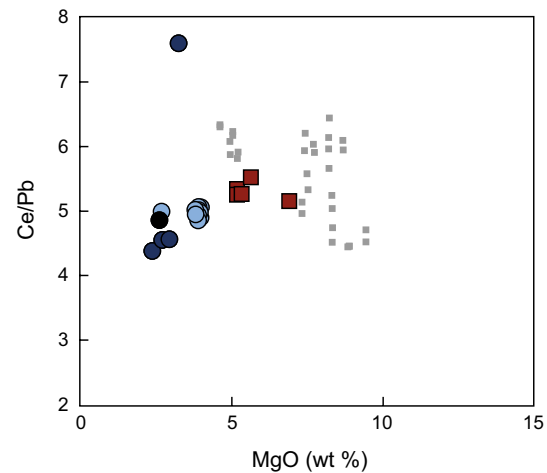
Fig. 10 Ce/Pb ratios for Bezymianny and Klyuchevskoy eruptive products. The Ce/Pb ratios are low and in the range of typical arc basalts (1–10: Miller et al. 1994; Noll et al. 1996; Plank 2005). Sediment addition from the subducted slab would impart a high Ce/Pb ratio; however, the Ce/Pb ratios between Bezymianny and Klyuchevskoy are similar. If the entire range of Klycuhevskoy published data is considered (*gray squares*), there is no discernable difference between Bezymianny and Klyuchevskoy Ce/Pb ratios

common process in arc magmas discussed extensively since Bowen (1928) and Daly (1933), and quantitatively explored by a number of papers (e.g., Taylor 1980; DePaolo 1981; Hildreth and Moorbath 1988; Reiners et al. 1995; Chiaradia et al. 2009; Dufek and Bergantz 2005). N-MORB normalized rare earth element patterns of the xenoliths are flat and depleted relative to all other samples of Bezymianny and N-MORB (Fig. 5) suggesting that these xenoliths may be samples of magmatic residues from the mid-crust. For one of these xenoliths (01BZT09b), we calculate a crystallization temperature and pressure of ~929 °C and 5.2 kbar (Online Resource 4). Because this sample of the crust has a Pb isotope signature less radiogenic than that of Bezymianny, assimilation of this material would cause Bezymianny magma compositions to shift away from Klyuchevskoy compositions. Therefore, some degree of the variable Pb isotope composition between Bezymianny and Klyuchevskoy may arise from assimilation of the mid-crust beneath Bezymianny.

To estimate the maximum degree of assimilation needed to reach the observed compositions, we modeled the behavior of Rb, Sr and Pb during deep crustal AFC (Fig. 11a–c, see Online Resource 5 for model parameters). The relatively unconstrained nature of AFC model parameters in the CKD does not justify a more complex formulation than the essential batch melting, assimilation and fractionation process we calculate here using equations of DePaolo (1981). A high-alumina basalt composition measured from Klyuchevskoy (Kersting and Arculus 1995) is used as the

initial magma because Bezymianny magmas likely evolve from such compositions (Ozerov et al. 1997). Simulations using MELTS (Ghiorso and Sack 1995) were conducted for both high-magnesium and high-aluminum CKD basalt compositions crystallizing at pressures between 5 and 7 kbar. The crystallizing assemblages from MELTS were coupled with the observed mineral assemblage in the metamorphosed crustal xenolith from this study to define a fractionating assemblage for the AFC model of 45 % clinopyroxene, 17 % orthopyroxene, 35 % plagioclase and 3 % magnetite. Appropriate partition coefficients were assigned to this fractionating assemblage (see Fig. 11 caption). Variation in Rb, Sr and Pb in the model is dependent on the concentrations of these elements in the assumed initial magma. Therefore, discrepancies between the model and the measured data may be a result of using a single high-alumina basalt from Kersting and Arculus (1995) that does not capture any natural variability. The composition of the crustal assimilant is taken from the mid-crustal xenolith from the 2007 eruption of Bezymianny. AFC models with $r = 0.9$ fit historical compositions well for Rb, Sr and Pb concentrations with only 5–10 % AFC (decrease in the fraction of remaining liquid of 5–10 %; Fig. 11). While this r value appears somewhat high, it is thermodynamically plausible given geophysical evidence for deep crustal melt beneath the KG. Because of the higher temperature of the lower crust at depths greater than 15 km, sensible heat consumption required to increase the wallrock temperature would be low and higher r values close to or equal to 1 are expected (DePaolo 1981). Reiners et al. (1995) also suggest that r values should be higher in the lower crust and decrease as AFC moves into the upper crust, and thermal models suggest that deep AFC occurs in arc settings (Dufek and Bergantz 2005; Annen et al. 2006). Until more constrained thermodynamic modeling of lower-crustal assimilation in young arcs is carried out, qualitative arguments allow for the plausibility of r values in the vicinity of 0.9. Older more evolved extrusive dome compositions at Bezymianny are best modeled by lower r values between 0.6 and 0.3 (Fig. 11) suggesting that prehistoric eruptions of Bezymianny may have undergone more shallow AFC (assuming that the initial magma and modes have not changed). This is consistent with the more evolved petrologic nature of these domes as well as with modern seismic tomography data showing that mid-crustal reservoirs beneath Bezymianny are transient (Koulakov et al. 2013).

Crustal assimilation and fractional crystallization at a depth of ~15–20 km beneath Bezymianny are consistent with other studies of the KG volcanoes. Ozerov et al. (1997) and Almeev et al. (2013b) propose a deep magma chamber beneath Bezymianny at depths similar to those we calculate for the mid-crustal xenolith (15–20 km).

Ozerov et al. (1997) also found Sr isotope evidence for minor assimilation at Bezymianny, though they do not account for this their modeling. Contrary to the Ozerov et al. (1997) model, which suggests that only fractional crystallization is required to evolve Klyuchevskoy magmas to Bezymianny compositions, high-precision Pb isotopes show that Bezymianny and Klyuchevskoy magmas do not compose a continuous differentiation sequence produced from a single source. Bezymianny magma compositions require at least some contributions from either lower-crustal assimilation or from magma mixing with less radiogenic mafic magmas.

Unique unradiogenic Pb isotope composition of the Klyuchevskoy group

While Bezymianny has less radiogenic Pb isotope compositions than Klyuchevskoy, more generally both of these volcanoes have less radiogenic Pb isotope compositions than Karymsky volcano to the south (Eastern Volcanic Front) and Shiveluch volcano to the north (Northern CKD) (Fig. 6). These data differ from Churikova et al. (2001) who report that Shiveluch Pb isotope compositions are comparable to the KG.

Amphibolite massif outcrops south of the CKD preserve evidence that the island arcs that accreted to form western Kamchatka are young (less than ~66 Ma; Bindeman et al. 2002). Unlike older continental arcs, the young lower crust beneath Kamchatka results in little contrast with the underlying mantle in Pb isotope compositions. Assuming a range of U/Pb ratios for the lower crust ($^{238}U/^{204}Pb = 2.1$–10), the $^{206}Pb/^{204}Pb$ ratio of the lower crust only increases by 0.16–0.56 % over 66 million years. The $^{206}Pb/^{204}Pb$ isotope composition of the lower-crustal inclusion from Bezymianny differs from Klyuchevskoy-like basalts by approximately 0.6 % and from Shiveluch magmas by ~1 %. Although the lower crust does not contrast strongly with juvenile magmas in Pb isotope composition, the differences are resolvable by high-precision Pb isotope analyses. Assimilation of lower crust beneath the entire KG may explain the unradiogenic compositions relative to Shiveluch and Karymsky volcanoes. Lower-crustal assimilation may be a pervasive process beneath KG with only subtle geochemical manifestations.

Mid- and lower-crustal magma residence beneath the KG is supported by geophysical evidence. Geophysical data do not resolve a sharp Moho beneath the KG; rather, the data image an approximately 12–14-km-thick region of slow seismic velocities between depths of 23 and 37 km (Balesta 1991; Lees et al. 2007; Koulakov et al. 2013). This observation is interpreted to represent a region with considerable proportions of partial melting and either

Fig. 11 AFC models to reproduce Bezymianny trace element and ▶ Pb isotope compositions. AFC paths calculated using the equations of DePaolo (1981) for the evolution of Rb, Sr and Pb in the melt are shown for *r* values of 0.9 (*black curve*), 0.6 (*dark gray curve*) and 0.3 (*light gray curve*). **a–c** The trace element behavior in the melt for a high-alumina basalt initial magma composition (Kersting and Arculus (1995): K-114, Rb = 15.6 ppm, Sr = 371 ppm, Pb = 4 ppm, 206Pb/204Pb = 18.280). The composition of the assimilant is taken from the mid-to-lower-crustal xenolith found in the 2007 eruption of Bezymianny (Rb = 5.85, Sr = 194.74, Pb = 1.49, 206Pb/204Pb = 18.183). The fractionating phase assemblage used was derived through MELTS (Ghiorso and Sack 1995) runs crystallizing Klyuchevskoy-like basalt between 5 and 7 kbar: 45 % clinopyroxene, 17 % orthopyroxene, 35 % plagioclase and 3 % magnetite. Partition coefficients are from the basalt–basaltic andesite compilation of Rollinson (1993) for Sr and Rb, and are from Hauri et al. (1994) for Pb in clinopyroxene, Dunn and Sen (1994) for Pb in orthopyroxene and plagioclase and from Ewart and Griffin (1994) for Pb in magnetite. Tick marks represent 5 % intervals of AFC (5 % changes in "F"—the fraction of remaining liquid—from 1 to 0.5). The data for Bezymianny eruptive products are modeled well with a high-alumina starting composition and 5–10 % lower-crustal AFC (*r* = 0.9). The more evolved domes require lower *r* values to fit the data (r between 0.6 and 0.3) consistent with an evolution in the shallow crust (see text for "Discussion"). Model parameters are summarized in Online Reference 5

magma storage in the lower crust or magma underplating the crust (Balesta 1991; Churikova et al. 2001; Lees et al. 2007; Koulakov et al. 2013). Regional surface deformation also supports the idea of a large sill-like magma body beneath the KG (Grapenthin et al. 2013). We hypothesize that this blurred Moho region represents ponding of rising magmas where regional baseline assimilation of the lower crust occurs beneath the KG. This process would also contribute to homogenization of any short-length scale isotopic heterogeneities inherited from the mantle source. Granulitic facies with unradiogenic Pb isotope compositions, similar to the crustal xenolith sampled by Bezymianny magma, may extend from depths greater than 15 km down to this region of partial melt. The unradiogenic Pb composition imparted through deep crustal assimilation is not observable along the arc outside of the KG.

Pb isotope variation over short timescales

In addition to isotopic contrast between Bezymianny and Klyuchevskoy volcanoes, we document changes in Pb isotope composition over both short (decadal) and longer time periods (e.g., the time difference between extrusive dome emplacement and the modern edifice of Bezymianny). Older Klyuchevskoy lavas (1939–1946) are less radiogenic than lavas from 2007 (Fig. 12a) and record compositional change in the very recent history of the volcano. On a longer timescale, the extrusive domes on the southern flank of Bezymianny are more radiogenic than modern
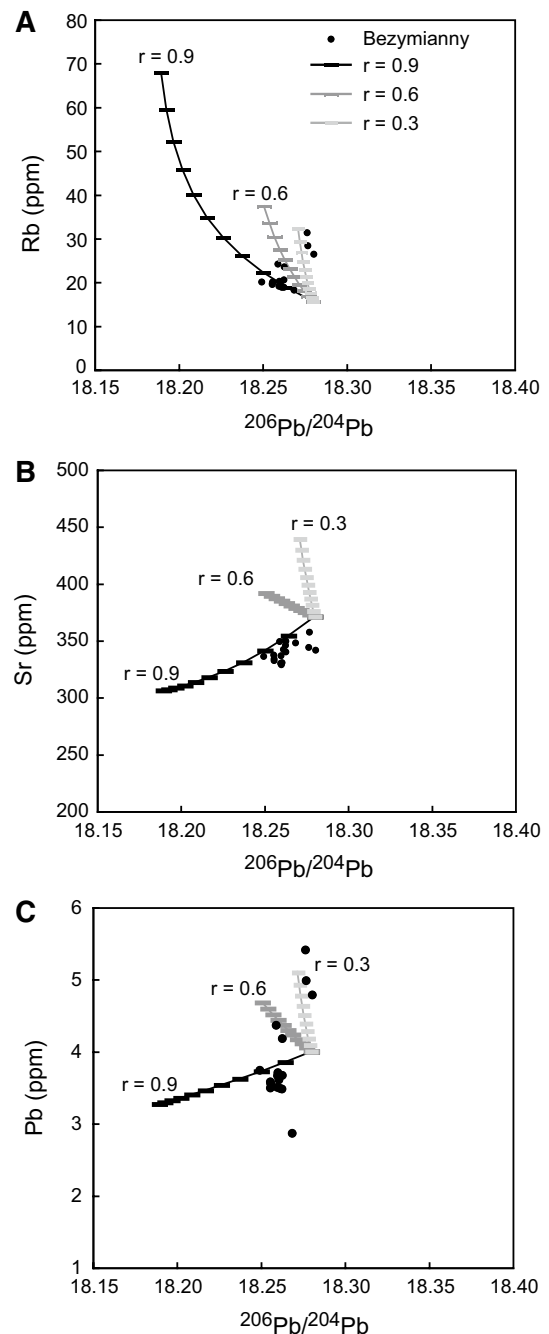
eruptions (1956–present; Fig. 12b). The extrusive domes at Bezymianny have not been dated but are estimated to be late Pleistocene and Holocene in age (Almeev 2005; Bogoyavlenskaya et al. 1991). The Pb isotope compositions of Bezymianny and Klyuchevskoy appear to diverge with time.

These shifts in isotopic composition suggest that either the sources of melt beneath the KG change rapidly (~ decades) or that the intensity of deep magmatic processes such as assimilation varies over short time periods. Variations

Fig. 12 Temporal Pb isotope variation at Bezymianny and Klyuchevskoy volcanoes. **a** Klyuchevskoy Pb isotope variation. Five different eruptive units from Klyuchevskoy are shown. The youngest lavas (2007) are more radiogenic than older flank lavas of Klyuchevskoy. **b** Bezymianny Pb isotope variation. The older extrusive domes at Bezymianny are more radiogenic than the 1956–2007 modern juvenile eruptive units
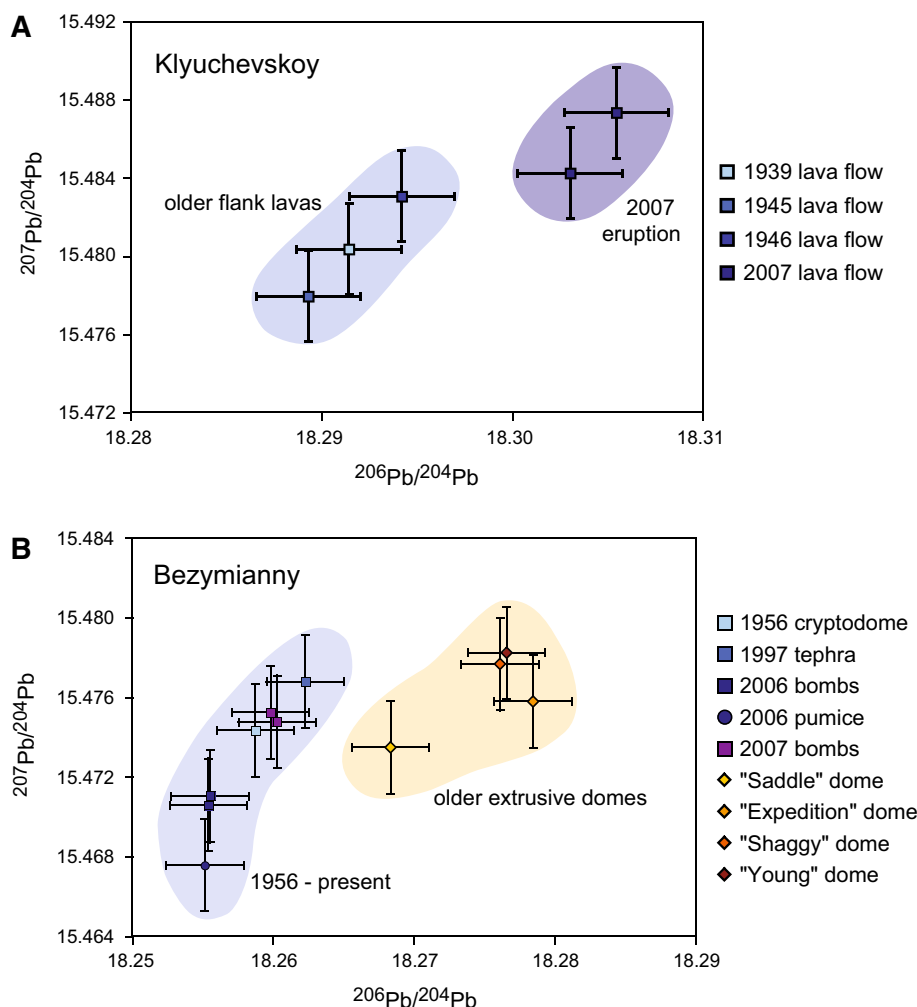
in the amount of crustal assimilation have been suggested to correspond to the non-steady-state eruptive history of Klyuchevskoy volcano during the Holocene (Portnyagin et al. 2011). The data that resolve decadal variability suggest that these processes change on much shorter timescales as well. The shift observed in Pb isotope compositions between Pleistocene–Holocene extrusive domes and 1956–present-day juvenile deposits shows that, only a few million years ago, magmas extruded at Bezymianny were distinctly more radiogenic (Fig. 12b). Shifts on these timescales at Bezymianny are reasonable; however, they must be much more rapid at Klyuchevskoy. Klyuchevskoy lavas vary in Pb isotope composition over a 60–70 year time frame, which requires changes in the magma source or the degree of assimilation on the order of decades.

Conclusions

The unradiogenic Pb isotope signature of Bezymianny relative to Klyuchevskoy volcano demonstrates that

Bezymianny magmas cannot be produced only by crystal fractionation of Klyuchevkoy-like magmas as previously hypothesized (Ozerov et al. 1997). Initial melts from the mantle source region beneath both Bezymianny and Klyuchevskoy may be similar in composition when they underplate the crust; however, magmas that erupt at Bezymianny have undergone either (1) mixing with a compositionally distinct magma and/or (2) have assimilated more mid- to lower-crustal material than those erupted at Klyuchevskoy (Fig. 13). High-precision Pb isotope data have the resolution to document the interaction of magmas with young mid-crust, a process that is not resolvable using only major or trace element compositions.

Less radiogenic Pb isotope compositions measured for the KG relative to magmas erupted in northern and southern Kamchatka suggest that deep crustal assimilation–fractional–crystallization (AFC) processes vary regionally and are more dominant beneath the KG. This geochemical inference is supported by the presence of a geophysically imaged thick blurred Moho indicating large amounts of mafic magma underplating the crust of the KG. In addition,
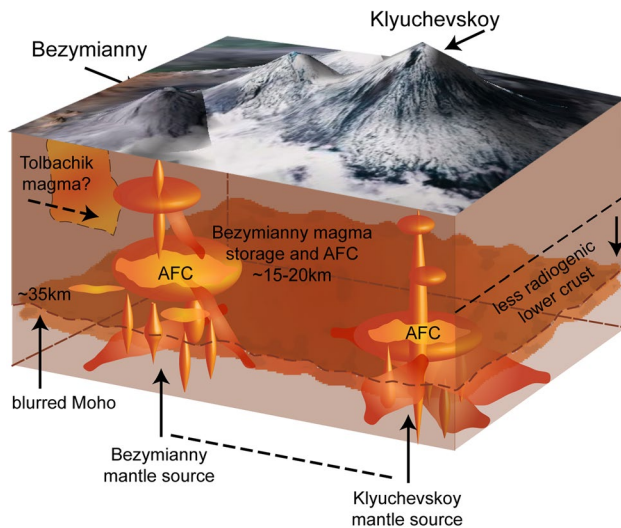
Fig. 13 New conceptual model for magma generation beneath Bezymianny and Klyuchevskoy volcanoes. Magmas generated in the mantle source regions beneath Bezymianny and Klyuchevskoy have similar compositions. The entire lower crust of the CKD is underplated with mafic magmas from the mantle at a depth of ~35 km (*blurred Moho arrow*; Balesta 1991; Lees 2007). All CKD magmas interact with the lower crust to some degree—this lower crust has a less radiogenic Pb isotope composition relative to mantle-derived magmas. Bezymianny magmas and Klyuchevskoy magmas take paths through the crust that are not connected to one another. Klyuchevskoy magmas experience some lower-crustal assimilation and fractional crystallization (AFC), but in general are transported through a well-developed vertical conduit system. Bezymianny magmas, however, undergo more extensive AFC processing in the lower crust (shown here with a larger region of deep AFC) and are stored at various depths in the *upper crust* [see Fedotov et al. (2010) and Koulakov et al. (2013) for crustal storage]. Bezymianny magmas also mix with more mafic melts unrelated to Klyuchevskoy that may feed Tolbachik volcano

variation in Pb isotope compositions beneath single volcanic centers in the KG suggests that the degree of assimilation can change over decadal timescales and on spatial scales less than 10 km.

In continental arc settings, lower-crustal AFC processes are documented by unambiguous geochemical excursions, such as clear amphibole signatures (Dy/Yb variation), or garnet signatures (high Sr/Y), accompanied by measurable isotopic shifts from assimilation of older crust (e.g., Gao et al. 2004). However, Kamchatka represents a class of arcs within which lower-crustal AFC processes, though they may be pervasive, are not geochemically obvious. In young, thin arcs with MORB-like isotopic compositions, lower-crustal AFC is typically cryptic (Reagan et al. 2003) or may go unobserved altogether. High-precision Pb isotope data from the Kamchatka arc suggest that in such arc settings, deep assimilation and magma mixing are important processes in the generation of erupted magmas.

References

Abouchami W, Hofmann AW, Galer SJG, Frey FA, Eisele J, Feigenson M (2005) Lead isotopes reveal bilateral asymmetry and vertical continuity in the Hawaiian mantle plume. Nature 434:851–856

Albarède F, Télouk P, Blichert-Toft J, Boyet M, Agranier A, Nelson BK (2004) Precise and accurate isotopic measurements using multiple-collector ICPMS. Geochim Cosmichim Acta 68:2725–2744

Almeev RR (2005) Geochemistry of Bezymianny volcano: evidence for mantle source and insights on fractionating parameters of the parental magmas, Ph.D Dissertation, Moscow State University, 238 pp (In Russian)

Almeev RR, Kimura J, Ariskin AA, Ozerov AY (2013a) Decoding crystal fractionation in calc-alkaline magmas from the Bezymianny Volcano (Kamchatka, Russia) using mineral and bulk rock compositions. J Volcanol Geotherm Res. doi:10.1016/j.jbolgeores.2013.01003

Almeev RR, Holtz F, Ariskin AA, Kimura J (2013b) Storage conditions of Bezymianny parental magmas: results of phase equilibria experiments at 100 and 700 MPa. Contrib Mineral Petrol 166:1389–1414

Annen C, Blundy JD, Sparks RSJ (2006) The genesis of intermediate and silicic magmas in deep crustal hot zones. J Petrol 47:505–539

Anosov GI, Bikkenina SK, Popov AA (1978) *Glubinnoe seismicheskoe zondirovanie Kamchatki* (Deep Seismic Sounding of Kamchatka), Moscow: *Nauka*, 129 pp (In Russian)

Arevalo R Jr, McDonough WF (2010) Chemical variations and regional diversity observed in MORB. Chem Geol 271:70–85

Ariskin AA, Barmina GS, Ozerov AYu, Nielsen RL (1995) Genesis of high-alumina basalts from Klyuchevskoi volcano. Petrology 3:449–472

Auer S, Bindeman I, Wallace P, Ponomareva V, Portnyagin M (2009) The origin of hydrous, high-$\delta18O$ voluminous volcanism: diverse oxygen isotope values and high magmatic water contents within the volcanic record of Klyuchevskoy volcano, Kamchatka, Russia. Contrib Mineral Petrol 157:209–230

Balesta ST (1991) Earth crust structure and magma chambers of the areas of present Kamchatka volcanism. In: Fedotov SA, Masurenkov YP, Balesta ST (eds) Active volcanoes of Kamchatka. Nauka, Moscow, pp 36–45

Belousov AB, Belousova MG, Zhdanova EYu (1996) Northern group of Kamchatkan volcanoes: activity in 1990–1992. J Volcanol Seismol 18:161–170

Belousov A, Voight B, Belousova M, Petukhin A (2002) Pyroclastic surges and flows from the 8–10 May 1997 explosive eruption of Bezymianny volcano, Kamchatka, Russia. Bull Volcanol 64:455–471

Bindeman I, Vinogradov VI, Valley JW, Wooden JL, Natal'in BA (2002) Archean protolith and accretion of crust in Kamchatka: SHRIMP dating of zircons from Sredinny and Ganal Massifs. J Geol 110:271–289

Bindeman IN, Ponomareva V, Bailey JC, Valley JW (2004) Volcanic arc of Kamchatka: a province with high-δ18O magma sources and large-scale $^{18}O/^{16}O$ depletion of the upper crust. Geochim Cosmichim Acta 68(4):841–865

Blichert-Toft J, Weis D, Maerschalk C, Agranier A, Albarède F (2003) Hawaiian hot spot dynamics as inferred from the Hf and Pb isotope evolution of Mauna Kea volcano. Geochem Geophys Geosyst 4. doi:10.1029/2002GC000340

Bogoyavlenskaya GY, Braitseva OA, Melekestsev IV, Maksimov AP, Ivanov BV (1991) Bezymianny volcano. In: Fedotov SA, Masurenkob YP (eds) Active volcanoes of Kamchatka. Nauka, Moscow, pp 168–197

Bowen NL (1928) The evolution of igneous rocks. Princeton University Press, Princeton

Braitseva OA, Melekestsev IV, Bogoyavlenskaya GE, Maksimov AP (1991) Bezymianny: eruptive history and dynamics. J Volcanol Seismol 12:165–194

Braitseva OA, Melekestsev IV, Ponomareva VV, Sulerzhitsky LD (1995) The ages of calderas, large explosive craters and active volcanoes in the Kuril-Kamchatka region, Russia. Bull Volcanol 57:383–402

Brenan JM, Shaw HF, Phinney DL, Ryerson FJ (1994) Rutile-aqueous fluid partitioning of Nb, Ta, Hf, Zr, U and Th: implications for high field strength element depletions in island-arc basalts. Earth Planet Sci Lett 128:327–339

Brunelli D, Seyler M (2010) Asthenospheric percolation of alkaline melts beneath the St. Paul region (Central Atlantic Ocean). Earth Planet Sci Lett 289:393–405

Chiaradia M, Müntener O, Beate B, Fontignie DA (2009) Adakite-like volcanism of Ecuador: lower crust magmatic evolution and recycling. Contrib Mineral Petrol 158:563–588

Churikova T, Dorendorf F, Wörner G (2001) Sources and fluids in the mantle wedge below Kamchatka, evidence from across-arc geochemical variation. J Petrol 42(8):1567–1593

Churikova TG, Gordeychik BN, Wörner G, Ivanov BV (2011) Variable fluids and mantle sources documented in the geochemistry of Kamen volcano and the Klyuchevskaya volcanic group. Japan Kamchatka Aleutian Subduction Processes Meeting Abstracts

Daly RA (1933) Igneous rocks and their origin. McGraw Hill, New York

Davidson J, Turner S, Handley H, Macpherson C, Dosseto A (2007) Amphibole "sponge" in arc crust? Geology 35:787–790

DePaolo DJ (1981) Trace element and isotopic effects of combined wallrock assimilation and fractional crystallization. Earth Planet Sci Lett 53:189–202

Dorendorf F, Weichert U, Wörner G (2000) Hydrated sub-arc mantle: a source for the Klyuchevskoy volcano, Kamchatka/Russia. Earth Planet Sci Lett 175:69–86

Dosseto A, Bourdon B, Joron J, Dupre B (2003) U–Th–Pa–Ra study of the Kamchatka arc: new constraints on the genesis of arc lavas. Geochim Cosmichim Acta 67:2857–2877

Dufek J, Bergantz GW (2005) Lower crustal magma genesis and preservation: a stochastic framework for the evaluation of basalt–crust interaction. J Petrol 142:113–132

Duggen S, Portnyagin M, Baker J, Ulfbeck D, Hoernle K, Garbe-Schönberg D, Grassineau N (2007) Drastic shift in lava geochemistry in the volcanic-front to rear-arc region of the Southern Kamchtkan subduction zone: evidence for the transition from slab surface dehydration to sediment melting. Geochim Cosmichim Acta 71:452–480

Dunn T, Sen C (1994) Mineral/matrix partition coefficients for orthopyroxene, plagioclase, and olivine in basaltic to andesitic systems: a combined analytical and experimental study. Geochim Cosmichim Acta 58:717–733

Ewart A, Griffin WL (1994) Application of proton-microprobe data to trace-element partitioning in volcanic-rocks. Chem Geol 117:251–284

Fedotov SA, Masurenkov YP, Balesta ST (eds) (1991) Active volcanoes of Kamchatka. Nauka, Moscow

Fedotov SA, Zharinov NA, Gontovaya LI (2010) The magmatic system of the Klyuchevskaya Group of volcanoes inferred from data on its eruptions, earthquakes, deformation, and deep structure. J Volcanol Seismol 4:1–33

Gao S, Rudnick RL, Yuan H, Liu X, Liu Y, Xy W, Ling W, Ayers J, Wang X, Wang Q (2004) Recycling lower continental crust in the North China Craton. Nature 432:892–897

Ghiorso MS, Sack RO (1995) Chemical mass transfer in magmatic processes. IV. A revised and internally consistent thermodynamic model for the interpretation and extrapolation of liquid-solid equilibria in magmatic systems at elevated temperatures and pressures. Contrib Mineral Petrol 119:197–212

Gorbatov A, Kostoglodov V, Suarez G, Gordeev E (1997) Seismicity and structure of the Kamchatka subduction zone. J Geophys Res 102:17883–17898

Grapenthin R, Freymueller JT, Serovetnikov SS (2013) Surface deformation of Bezymianny Volcano, Kamchatka, recorded by GPS: the eruptions from 2005 to 2010 and long-term, long-wavelength subsidence. J Volcanol Geotherm Res 263:58–74

Hart SR (1984) A large-scale anomaly in the Southern Hemisphere mantle. Nature 309:753–757

Hauri EH, Wagner TP, Grove TL (1994) Experimental and natural partitioning of Th, U, Pb and other trace elements between garnet, clinopyroxene and basaltic melts. Chem Geol 117: 149–166

Hildreth W, Moorbath S (1988) Crustal contributions to arc magmatism in the Andes of central Chile. Contrib Mineral Petrol 98:455–489

Hochstaedter AG, Kepezhinskas P, Defant M (1996) Insights into the volcanic arc mantle wedge from magnesian lavas from the Kamchatka arc. J Geophys Res 101(B1):697–712

Hofmann AW (1988) Chemical differentiation of the Earth: the relationship between mantle, continental crust, and oceanic crust. Earth Planet Sci Lett 90:297–314

Hofmann AW (1997) Mantle geochemistry: the message from oceanic volcanism. Nature 385:219–229

Ishikawa T, Tera F, Nakazawa T (2001) Boron isotope and trace element systematics of the three volcanic zones in the Kamchatka arc. Geochim Cosmichim Acta 65(24):4523–4537

Izbekov PE, Neill OK, Shipman JS, Turner SJ, Shcherbakov VD, Plechov P (2010) Silicic enclaves in products of 2009-2010 eruptions of Bezymianny volcano, Kamchatka: Implications for magmatic processes. AGU Fall Meeting Supplemental Abstract

Johnson DM, Hooper PR, Conrey RM (1999) XRF analysis of rocks and minerals for major and trace elements on a single low dilution Li-tetraborate fused bead. Adv X Ray Anal 41:843–867

Kamenov GD, Mueller PA, Perfit MR (2004) Optimization of mixed Pb–Tl solutions for high precision isotopic analyses by MC–ICP–MS. J Anal Atom Spectrom 19:1262–1267

Kelemen PB, Yogodzinski GM, Scholl DW (2003) Along strike variation in the Aleutian island arc: genesis of high-Mg# andesite and implications for continental crust. In: Eiler J (ed) Inside the subduction factory. Geophysical Monograph, American Geophysical Union, vol 138, pp 223–276

Kepezhinskas P, McDermott F, Defant MJ, Hochstaedter A, Drummond MS, Hawkesworth CJ, Koloskov A, Maury RC, Bellon H (1997) Trace element and Sr–Nd–Pb isotopic constraints on a three-component model of Kamchatka Arc petrogenesis. Geochim Cosmichim Acta 61(3):577–600

Kersting AB, Arculus RJ (1994) Klyuchevskoy volcano, Kamchatka, Russia: the role of high-flux recharged, tapped, and fractionated magma chamber(s) in the genesis of high-Al_2O_3 from high-MgO basalt. J Petrol 35:1–41

Kersting AB, Arculus RJ (1995) Pb isotope composition of Klyuchevskoy volcano, Kamchatka and North Pacific sediments: implications for magma genesis and crustal recycling in the Kamchatkan arc. Earth Planet Sci Lett 136:133–148

Khrenov AP, Dvigalo VN, Kirsanov IT, Fedotov SA, Gorel'chik VI, Zharinov NA (1991) Klyuchevskoy Volcano. In: Fedotov SA, Masurenkob YP (eds) Active volcanoes of Kamchatka. Nauka, Moscow, pp 106–153 (in Russian and English)

Khubanaya SA, Sobolev AV (1998) Primary melts of calc-alkaline magnesian basalts from the Klyuchevskoi volcano, Kamchatka. Dokl Earth Sci 360:537–539

Khubanaya SA, Bogoyavlenskiy SO, Novogorodtseva TA, Okrugina AI (1994) The mineralogy of the Klyuchevskoi magnesian basalts depicting the fractionation in the magma chamber. J Volcanol Seismol 3:315–338 (in Russian)

Konstantinovskaia EA (2001) Arc-continent collision and subduction reversal in the Cenozoic evolution of the Northwest pacific: an example from Kamchatka (NE Russia). Tectonophysics 333:75–94

Koulakov I, Gordeev EI, Dobretsov NI, Vernikovsky VA, Sunyukov S, Jakovlev A, Jaxybulatov K (2013) Rapid changes in magma storage beneath the Klyuchevskoy group of volcanoes inferred from time-dependent seismic tomography. J Volcanol Geotherm Res 263:75–91

Lees JM (2007) Seismic tomography of magmatic systems. J Volcanol Geotherm Res 167:37–56

Lees JM, VanDecar J, Gordeev E, Ozerov A, Brandon M, Park J, Levin V (2007) Three dimensional images of the Kamchatka-Pacific plate cusp. Kamchatka Geophys Monogr Seri Am Geophys Union 172:65–75

Lopez T, Ushakov S, Izbekov P, Tassi F, Cahill C, Neill O, Werner C (2013) Constraints on magma processes, subsurface conditions, and total volatile flux at Bezymianny Volcano in 2007–2010 from direct and remote volcanic gas measurements. J Volcanol Geoth Res 263:92–107

Madureira P, Mata J, Mattielli N, Queiroz G, Silva P (2011) Mantle source heterogeneity, magma generation and magmatic evolution at Terceira Island (Azores archipelago): constraints from elemental and isotopic (Sr, Nd, Hf, and Pb) data. Lithos 126:402–418

Melekestsev IV, Khrenov AP, Kozhernyaka NN (1991) Tectonic position and general description of volcanoes of Northern group and Sredinny Range. In: Fedotov SA, Masurenkob YP (eds) Active volcanoes of Kamchatka. Nauka, Moscow, pp 74–81

Miller DM, Goldstein SL, Langmuir CH (1994) Cerium/lead and lead isotope ratios in arc magmas and the enrichment of lead in the continents. Nature 368:514–519

Minster JB, Jordan TH (1978) Present-day plate motions. J Geophys Res 83:5331–5354

Mironov NL, Portnyagin MV (2011) H_2O and CO_2 in parental magmas of Kliuchevskoi volcano inferred from study of melt and fluid inclusions in olivine. Russ Geol Geophys 52:1353–1367

Mironov NL, Portnyagin MV, Pletchov PYu, Khubunaya SA (2001) Kamchatka: evidence from melt inclusions in minerals of high-alumina basalts. Petrology 9(1):46–62

Münker C, Wörner G, Yogodzinski G, Churikova T (2004) Behaviour of high field strength elements in subduction zones: constraints from Kamchatka–Aleutian arc lavas. Earth Planet Sci Lett 224:275–293

Noll PD, Newsom HE, Leeman WP, Ryan JG (1996) The role of hydrothermal fluids in the production of subduction zone magmas: evidence from siderophile and chalcophile trace elements and boron. Geochim Cosmichim Acta 60:587–611

Ozerov AY (2000) The evolution of high-alumina basalts of the Klyuchevskoy volcano, Kamchatka, Russia, based on microprobe analyses of mineral inclusions. J Volcanol Geotherm Res 95:65–79

Ozerov AY, Ariskin AA, Kyle P, Bogoyavlenskaya GE, Karpenko SF (1997) Petrological–geochemical model for genetic relationships between basaltic and andesitic magmatism of Klyuchevskoi and Bezymyannyi volcanoes, Kamchatka. Petrology 5:550–569

Ozerov AY, Firstov PP, Gavrilov VA (2007) Periodicities in the dynamics of eruptions of Klyuchevskoi volcano, Kamchatka. Kamchatka Geophys Monogr Ser Am Geophys Union 172:283–291

Pineau F, Semet MP, Grassineau N, Okrugin VM, Javoy M (1999) The genesis of the stable isotope (O, H) record in arc magmas: the Kamchatka's case. Chem Geol 135:93–124

Plank T (2005) Constraints from thorium/lanthanum on sediment recycling at subduction zones and the evolution of the continents. J Petrol 46:921–944

Plechov PYu, Tsai AE, Shcherbakov VD, Dirksen OV (2008) Opacitization conditions of hornblende in Bezymyannyi volcano andesites (March 30, 1956 eruption). Petrology 16:19–35

Portnyagin M, Manea VC (2008) Mantle temperature control on composition of arc magmas along the Central Kamchatka Depression. Geology 36:519–522

Portnyagin MV, Ponomareva VV (2012) Kliuchevskoy volcano diary. Int J Earth Sci 101:195

Portnyagin M, Hoernle K, Avdeiko G, Hauff F, Werner R, Bindeman I, Uspensky V, Garbe-Schoenberg D (2005) Transition from arc to oceanic magmatism at the Kamchatka–Aleutian junction. Geology 33:25–28

Portnyagin M, Hoernle K, Plechov P, Mironov N, Khubunaya S (2007a) Constraints on mantle melting and composition and nature of slab components in volcanic arcs from volatiles (H_2O, S, Cl, F) and trace elements in melt inclusions from the Kamchatka Arc. Earth Planet Sci Lett 255:53–69

Portnyagin M, Bindeman I, Hoernle K, Hauff F (2007b) Geochemistry of primitive lavas of the Central Kamchatka Depression: magma generation at the edge of the Pacific Plate. Kamchatka Geophys Monogr Ser Am Geophys Union 172:199–239

Portnyagin M, Mironov N, Ponomareva V, Bindeman I, Hauff F, Sobolev A, Kayzar T, Garbe-Schonberg D, Hoernle K (2011) Arc magmas from slab to eruption: the case of Kliuchevskoy volcano. Goldschmidt Conf Abstr 75:1661

Putirka KD (2008) Thermometers and barometers for volcanic systems. Rev Mineral Petrol 69:61–120

Reagan MK, Sims KWW, Erich J, Thomas RB, Cheng H, Edwards RL, Laybe G, Ball L (2003) Time-scales of differentiation from mafic parents to rhyolite in North American continental arcs. J Petrol 44:1703–1726

Regelous M, Hofmann AW, Abouchami W, Galer SJG (2003) Geochemistry of lavas from the Emperor Seamounts, and the geochemical evolution of Hawaiian magmatism from 85 to 42 Ma. J Petrol 44:113–140

Reiners PW, Nelson BK, Ghiorso MS (1995) Assimilation of felsic crust by basaltic magma—thermal limits and extents of crustal contamination of mantle-derived magmas. Geology 23(6):563–566

Rollinson HR (1993) Using geochemical data: evaluation, presentation, interpretation. Routledge, New York

Salters VJM, Stracke A (2004) Composition of the depleted mantle. Geochem Geophys Geosyst 5. doi:10.1029/2003GC000597

Shcherbakov VD, Plechov PY, Izbekov PE, Shipman JS (2011) Plagioclase zoning as an indicator of magma processes at

Bezymianny Volcano, Kamchatka. Contrib Mineral Petr 162:83–99

Shcherbakov VD, Neill OK, Izbekov PE, Plechov PY (2013) Phase equilibria constraints on pre-eruptive magma storage conditions for the 1956 eruption of Bezymianny Volcano, Kamchatka, Russia. J Volcanol Geoth Res 263:132–140

Shipman JS, Turner SJ, Gavrilenko M, Izbekov PE (2010) Rapid modal analysis and whole-rock geochemistry of the 1956–present eruptive products of Bezymianny volcano. AGU Fall Meeting Supplemental Abstract

Spiegelman M, Kelemen PB (2003) Extreme chemical variability as a consequence of channelized melt transport. Geochem Geophys Geosyst 4. doi:10.1029/2002GC000336

Stolper E, Newman S (1994) The role of water in the petrogenesis of Mariana trough magmas. Earth Planet Sci Lett 121:293–325

Sun S-s, McDonough WF (1989) Chemical and isotopic systematics of oceanic basalts: implications for mantle composition and processes. In: Saunders AD, Norry MJ (eds) Magmatism in the Ocean Basins, Geological Society Special Publication No. 42, pp 313–345

Tatsumi Y (2000) Slab melting: its role in continental crust formation and mantle evolution. Geophy Res Lett 27:3941–3944

Taylor HP (1980) The effects of assimilation of country rocks by magmas on $^{18}O/^{16}O$ and $^{87}Sr/^{86}Sr$ systematics in igneous rocks. Earth Planet Sci Lett 47:243–254

Todt W, Cliff RA, Hanser A, Hofmann AW (1996) Evaluation of a ^{202}Pb–^{205}Pb double spike for high-precision lead isotope analysis. In: Basu A, Hart SR (eds) Earth processes: reading the isotopic code. American Geophysical Union, Washington, DC, pp 429–437

Tolstykh ML, Naumov VB, Babansky AD, Bogoyavlenskaya GE, Khubunaya SA (2003) Chemical composition, volatile components, and trace elements in andesitic magmas of the Kurile–Kamchatka region. Petrology 5:407–425

Tsvetkov AA, Gladkov NG, Volynets ON (1989) Problem of sediment subduction and 10Be isotope in lavas of Kuril Islands and Kamchatka Peninsula. Translated from USSR Academy of Sciences 306:1220–1225

Turner S, McDermott F, Hawkesworth C, Kepezhinskas P (1998) A U-series study of lavas from Kamchatka and the Aleutians: constraints on source composition and melting processes. Contrib Mineral Petrol 133:217–234

Turner S, Sims KWW, Reagan M, Cook C (2007) A ^{210}Pb–^{226}Ra–^{230}Th–^{238}U study of Klyuchevskoy and Bezymianny volcanoes, Kamchatka. Geochim Cosmichim Acta 71:4771–4785

Turner SJ, Izbekov PI, Langmuir C (2013) The magma plumbing system of Bezymianny Volcano: insights from trace element whole-rock geochemistry and amphibole compositions. J Volcanol Geotherm Res 263:108–121

Volynets ON, Babanskii AD, Gol'tsman (2000) Variations in isotopic and trace-element composition of lavas from volcanoes of the Northern Group, Kamchatka, in relation to specific features of subduction. Geochem Int 38:974–989

Volynets A, Churikova T, Woerner G, Gordeychik BN, Layer P (2010) Mafic late Miocene-quaternary volcanic rocks in the Kamchatka back arc region: implications for subduction geometry and slab history at the Pacific-Aleutian junction. Contrib Mineral Petrol 159:659–687

Watson BF, Fujita K (1985) Tectonic evolution of Kamchatka and the sea of Okhotsk and implications for the Pacific Basin. In: Howell DG (ed) Tectonostratigraphic Terranes, AAPG, pp 333–348

Weis D, Kieffer B, Maerschalk C, Pretorius W, Barling J (2005) High-precision Pb–Sr–Nd–Hf isotopic characterization of USGS BHVO-1 and BHVO-2 reference materials. Geochem Geophys Geosyst 6. doi:10.1029/2004GC000852

White WM, Albarède F, Télouk P (2000) High-precision analysis of Pb isotope ratios by multi-collector ICP–MS. Chem Geol 167:257–270

Washington State University (WSU) Geoanalytical Laboratory http://www.sees.wsu.edu/Geolab/note.html

Yogodzinski GM, Lees JM, Churikova TG, Dorendorf F, Woerner G, Volynets ON (2001) Geochemical evidence for the melting of subducting oceanic lithosphere at plate edges. Nature 409:500–503